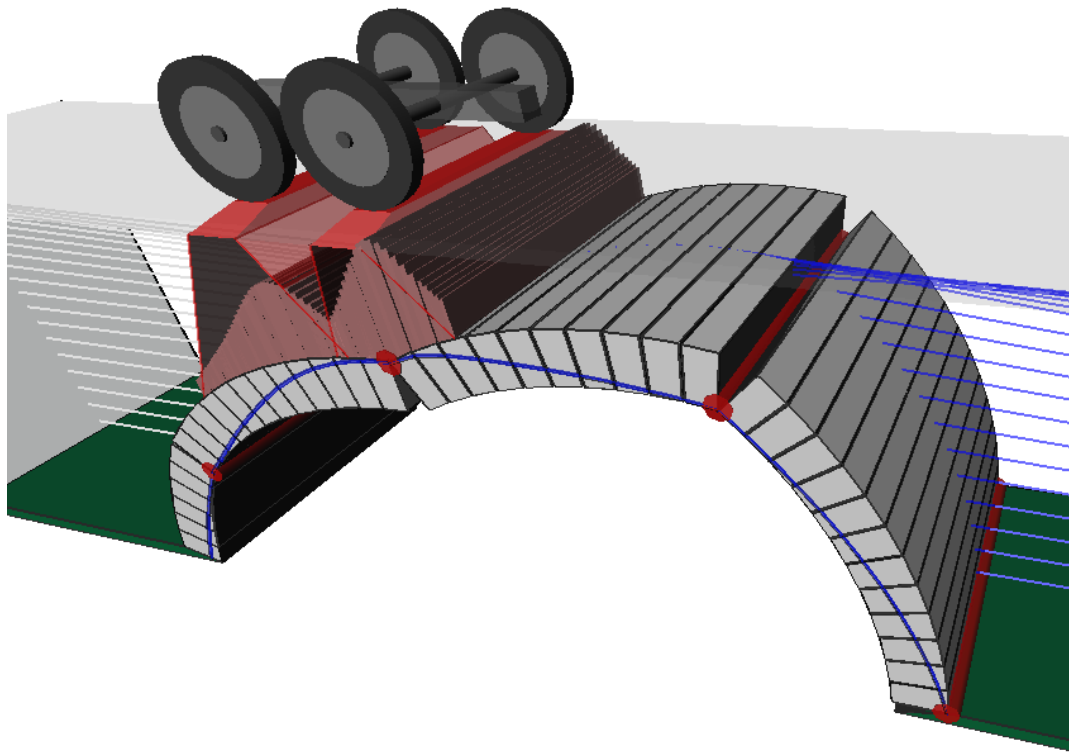


# CHALMERS



## On engineering methods for assessment of load capacity of stone arch bridges

Master's Thesis in the Master's programme Solid and Fluid Mechanics

**KRISTOFFER HOLMSTRÖM**

Department of Applied Mechanics  
*Division of Material and Computational Mechanics*  
CHALMERS UNIVERSITY OF TECHNOLOGY  
Göteborg, Sweden 2010  
Master's Thesis 2010:42



MASTER'S THESIS 2010:42

# On engineering methods for assessment of load capacity of stone arch bridges

Master's Thesis in the Master's programme Solid and Fluid Mechanics

KRISTOFFER HOLMSTRÖM

Department of Applied Mechanics  
*Division of Material and Computational Mechanics*  
CHALMERS UNIVERSITY OF TECHNOLOGY  
Göteborg, Sweden 2010

On engineering methods for assessment of load capacity of stone arch bridges

Master's Thesis in the Master's programme Solid and Fluid Mechanics  
KRISTOFFER HOLMSTRÖM

© KRISTOFFER HOLMSTRÖM, 2010

Master's Thesis 2010:42

ISSN 1652-8557

Department of Applied Mechanics

Division of Material and *Computational Mechanics*

Chalmers University of Technology

SE-412 96 Göteborg

Sweden

Telephone: + 46 (0)31-772 1000

Cover:

Simulation of a bogie load on a stone arch bridge made in the program RING2.0.

Name of the printers / Department of Applied Mechanics  
Göteborg, Sweden 2010

On engineering methods for assessment of load capacity of stone arch bridges

Master's Thesis in the Master's programme Solid and Fluid Mechanics

KRISTOFFER HOLMSTRÖM

Department of Applied Mechanics

*Division of Material and Computational Mechanics*

Chalmers University of Technology

## ABSTRACT

Almost 800 stone arch bridges are in use on the Swedish national rail and road networks. These old structures were designed to carry a considerably smaller load than what is the load on railways or roads today. Today the stone arch bridges on the road network are assessed using inspections and on the rail network are assessed using inspections/calculations. To be able to calculate the load capacity of a stone arch bridge there are a number of different methods in the literature to use. Some of these are presented as a part of this thesis. Two commercial programs for calculations of load capacity of stone arch bridges are RING2.0 and Archie-M. Both programs have been used in this work to calculate the load capacity on two bridges, one long span bridge and one with a shorter span. A parametric study have been performed to identify material parameters that have a large influence on the load capacity. The realistic interval of each parameter have been found in the literature. The purpose of the parametric survey is also to compare computational results for both commercial programs. It was found that the fill height was the most influential parameter on the load capacity. For the short span bridge the angle of friction for the backfill material also played a significant role in RING2.0. The comparison of the two commercial programs shows that Archie-M gives a lower load capacity than RING2.0 for the cases tested.

Keywords: Stone arch, masonry arch, bridge load capacity, RING2.0, Archie-M,

Om ingenjörsmetoder för bärlighetsberäkningar av stenvalv

Examensarbete inom Solid and fluid mechanics

KRISTOFFER HOLMSTRÖM

Institutionen för tillämpad mekanik

*Avdelningen för Material och Beräkningsmekanik*

Chalmers tekniska högskola

## SAMMANFATTNING

Nästan 800 stenvalvsbroar är idag i bruk på de nationella väg- och järnvägsnäten. Dessa gamla byggnadsverk var konstruerade för att tåla betydligt mindre laster än vad de utsätts för idag. Det finns därför ett behov att klassningsberäkna dessa broar. Idag så är stenvalvsbroarna på vägnätet bedömda genom inspektioner och på järnvägsnätet genom inspektioner/beräkningar. För att beräkna lastkapaciteten på en stenvalvsbro finns det flertalet metoder, några av dessa kommer att presenteras genom en litteratur studie. Två kommersiella program för beräkningar av stenvalvsbroar är RING2.0 och Archie-M. Båda dessa program har använts för att beräkna lastkapaciteten på två stenvalvsbroar, en med stort spann och en med ett mindre spann. En parameterstudie med parameterintervall hämtade från litteraturen har genomförts för att identifiera kritiska parametrar för lastkapaciteten. Genom denna parameterstudie har också beräkningsresultaten från de båda programmen kunnat jämföras.

Den parameter som hade störst inflytande på lastkapaciteten var fyllnadshöjden. För stenvalvsbron med ett kort spann spelade även fyllnadsmaterialets friktionsvinkel en betydande roll i RING2.0. Jämförelsen mellan de båda kommersiella programmen visar att Archie-M ger en lägre beräknad lastkapacitet än RING2.0 i de jämförda fallen..

Nyckelord: Stenvalv, murverksbåge, bärlighetsberäkning, RING2.0, Archie-M.

# Contents

ABSTRACT	I
SAMMANFATTNING	II
CONTENTS	III
PREFACE	V
NOTATIONS	VI
1 INTRODUCTION	1
1.1 Background	1
1.2 Purpose	1
2 ASSESSMENT OF MASONRY ARCH BRIDGES IN SWEDEN TODAY	2
2.1 Design codes and regulations	2
2.1.1 A historical note	3
2.2 Inspection	4
3 ARCHES	6
3.1 Masonry arch - construction and concepts	6
3.2 Arches in history	8
3.3 Masonry arch mechanics	10
3.3.1 Assumptions	10
3.3.2 The funicular polygon	10
3.4 The line of thrust	13
3.5 The middle third rule	13
3.6 Pippard's elastic method	14
4 METHODS OF CALCULATING LOAD CARRYING CAPACITY – AN OVERVIEW	18
4.1 The MEXE method	18
4.2 Thrust line analysis	20
4.3 Thrust zone analysis	20
4.4 Mechanism method	21
4.5 Finite Element Methods	22
4.5.1 Frame analysis	22
4.5.2 Two and three dimensional FEM	23
4.6 Discrete Element Method	24
4.7 Commercial software: RING2.0	26
4.8 Commercial software: Archie-M	27

5	COMPARISON OF DIFFERENT CALCULATION METHODS	–
	LITERATURE SURVEY	28
5.1	Test results	28
5.2	Computations compared with tests	28
5.2.1	The MEXE method	28
5.2.2	FEM using tapered beam element	29
5.2.3	3D FEM – ABAQUS	29
5.2.4	RING	30
5.2.5	UDEC	31
5.3	Comparison of computational methods	32
5.3.1	FEM, RING and Archie-M	32
5.3.2	UDEC and RING2.0	33
5.3.3	ANSYS and 3DEC	33
6	PARAMETRIC STUDY – INFLUENCE OF DIFFERENT MATERIAL PARAMETERS ON THE LOAD CARRYING CAPACITY	35
6.1	Material parameters	35
6.1.1	Arch barrel	35
6.1.2	Backfill	37
6.1.3	Arch geometries	39
6.1.4	Loading	40
6.2	Parametric survey	41
6.2.1	Method	41
6.2.2	Results	43
6.2.3	Compilation of results	53
7	CAPACITY CALCULATION USING DESIGN CODE STANDARD VEHICLES	55
7.1	Damages	56
8	CONCLUSIONS	58
8.1	Preferable method of load carrying calculation	58
8.2	Crucial parameters of assessment	58
9	REFERENCES	60

# Preface

This thesis was initiated by WSP Samhällsbyggnad and the work has been carried out at their office in Karlstad. I would like to thank my supervisor Ola Lagerkvist , Göran Werme and Per Maxstadh for their help and support during my thesis work.

I would also like to thank my supervisor and examiner Mats Ander for his invaluable support and guidance and all the time he has spent helping me.

At last I would like to thank the software manufacturers LimitState and Obvis for making it possible to use their programs for this master's thesis.

Karlstad, May 2010

Kristoffer Holmström

# Notations

Notations are explained in the order they appear.





# 1 Introduction

## 1.1 Background

For ages man have had the ambition to overcome obstacles in the terrain. The first bridges may have been just a tree that had fallen over a stream. As the development proceeded more complicated bridges were constructed and for a long time a stone or masonry arch was the most robust and durable construction of a bridge. Time went on and steel, reinforced concrete and mixtures of these competed out the stone and masonry arches. But due to the durability of the material and the good ability to withstand the passage of time there are still many of these masonry arch bridges in use.

The problem is that it is not just the development of construction that has proceeded. Cars, trucks, trains and other vehicles that use the bridges have become much heavier in a way that no one could imagine when the bridges were constructed. This increase in load results in a need to assess the load carrying capacity of the bridge in order to use the bridge for full traffic load.

## 1.2 Purpose

The way to assess the load carrying capacity of stone or masonry arch bridges is no exact science. There are many variables that have to be taken into account and where perhaps none is known. Which materials are used, how is the arch constructed, what properties has the backfill, the ground and much more are all example of things that need to be considered and to which the answer can be all but clear.

However, there are various methods that can be used in the assessment of stone and masonry arch bridges. The purpose of this master thesis is to investigate methods of assessing masonry arches, compare them and present a good way to make control calculations and determine the allowed traffic load.

## 2 Assessment of masonry arch bridges in Sweden today

On the Swedish rail network there are 3620 bridges. Out of those there are 150 arch bridges, 115 with a stone arch, 35 with a concrete arch and no one with an arch made out of bricks. Sustainable bridges (2004)

The national Swedish road administration has 15817 bridges on the Swedish roads. Out of those there are 993 arch bridges 267 concrete-, 42 steel- and 684 stone-arches. Vägverket (2010[2])

An example of a stone arch bridge on the Swedish road system is seen in Figure 2.1. The bridge is a two span stone arch built 1870 located outside Eslöv. In the publication over culturally valuable bridges there are many stone arch bridges that are considered culturally valuable and that should be preserved. Vägverket (2005).

With a total of 799 stone arch bridges and many of them considered culturally valuable there is a need to assess these to be able to preserve them.



*Figure 2.1 Stone arch bridge over Bråån outside Eslöv. Vägverket (2005).*

### 2.1 Design codes and regulations

Although there are quite a few arch bridges in Sweden there are very few design codes and regulations regarding them.

The Swedish Rail Administration has a section in BVS 583.11 that defines a series of material parameters that can be used for analysis of stone arches. The specified parameters can be seen in Table 2.1. The compressive strength and Young's modulus is stated in the code. But the bridge must be inspected during the assessment. If the results from the inspection imply that other material parameters than what is stated in

the code is suitable for the current bridge, the values from the inspection should be used. The code also defines the minimum of parameters to take into account in an inspection. Banverket (2005)

*Table 2.1 Material parameters for stone arch bridges, from the Swedish Rail Administration*

Voussoir stones			Mortar material		
Compressive strength	300	MPa	Compressive strength and Young's modulus according to class C12/15		
Young's modulus	66	GPa	Tensile strength	0	MPa
Coefficient of friction between voussoir stone and mortar material					0,5
Partial coefficient in ultimate limit state (ULS) for compressive strength					1,5
Partial coefficient in ULS for Young's modulus					1,2

The Swedish Road Administration has a regulation for rating calculation of road bridges. This is not valid for bridges that have a load carrying structure made of stone and it does not give any other suggestion of ways to calculate load carrying capacity. Vägverket (1998)

### **2.1.1 A historical note**

This section is based upon an old publication signed in Stockholm March 1918 by a man named Leopold Abel, who after some research was found to (probably) have been an engineer at the Royal Railway Board of Building (Kungliga Järnvägsstyrelsens byggnadsbyrå). This document gives a glimpse of the regulations that controlled building for about a hundred years ago and should be seen more as a curiosity than anything else.

The publication states that all masonry work should be made out of granite that is in good shape and that is frost-resistant. The granite in arch and spandrel wall should have a minimum compressive strength of  $1500 \text{ kg/cm}^2$ . Mortar material should be made out of Swedish portland cement and sharp edged gravel. After 28 days of hardening the mortar should have a compressive strength of  $250 \text{ kg/cm}^2$  and a tensile strength of  $20\text{-}25 \text{ kg/cm}^2$ .

It is interesting to note that the old instructions gave the possibility to utilize the tensile strength of the mortar material for design of the bridge, something that is not allowed today.

## 2.2 Inspection

The Swedish road administration has not any specifications of what an inspection should include. Jonas Bergsten, who is a bridge technician at the Swedish road administration, has presented some points that they look for at an inspection. These are for example:

- What is the shape of the arch?
- Are there any loose stones in the arch or spandrels?
- Have there been any movements, settlings etc.?
- Have movements created cracking of stones in the arch?
- What shape and size are the stones?
- What is the fill height?
- What kind of foundation are the bridge built on?
- Have growth of plants affected the bridge?

The inspection is led by “people with long experience” and the results are gathered for a final judgement where current allowed traffic loading also is included. If the results show that the new allowed traffic load is not enough, actions are proposed to increase the load carrying capacity.<sup>1</sup>

The Swedish Rail administration has in *BVS 583.11* stipulated some points that should be checked during an inspection. These are:

- Symmetry of the arch
- Dilatations of joints
- Cracks in stone (granite) or joints
- Lime leaching
- Fill height
- Foundation

Also, as said, should an assessment be made whether the material parameters assumed in Table 2.1 are reasonable or not considering arch condition and shape.

---

<sup>1</sup> Bergsten, Jonas (2010-03-08) Bridge technician, Vägverket

## 2.3 Computations

The Swedish Rail administration stipulates that computations of a stone arch should be made using beam elements where the joints between the elements are placed in the centre line of the real arch. Banverket (2005)

The computed cross sectional forces should be compared to the characteristic values for the mortar material. The position of the line of thrust must also be checked. Banverket (2005)

### 3 Arches

The history of arches is long and spans from early Sumerian work in dried mud bricks to today's slender reinforced concrete arches. ICE (2008) Material and practices have changed but the arch is still a good way of reaching over long spans in just one or few leaps. The shape of the arch gives mainly compressive stresses which are needed for masonry and stone constructions where tensile forces can't be handled. Samuelsson A. Wiberg N-E. (1995)

#### 3.1 Masonry arch - construction and concepts

For a stone or masonry arch bridge the foundation is critical. Large thrusts from the arch needs to be transferred down to keep the arch in position. Preferably the arch foundation should therefore be made on solid rock, but this may not always be possible. Many techniques have been used, e.g. timber piling, faggots or just simply nothing. Lots of bridges have failed during the years so the stone and masonry arches we can see today are the top of the line concerning foundation. ICE (2008)

On the foundation, called skewback or abutment, the arch is erected. For this purpose a falsework, or centering, made of timber is constructed that can support the arch during construction. Figure 3.1 shows such a centering. Heyman (1982)



*Figure 3.1 Centering for an unknown bridge in Connecticut. Connecticut's historic highway bridges (2010)*

Upon the centering the arch is built, see Figure 3.2.



*Figure 3.2 Bulkeley Bridge, Connecticut, under construction. Connecticut's historic highway bridges (2010)*

Once the last stone, the keystone, is inserted into the arch the falsework can be removed. During the removal, fill must be put on the arch for stability and this need to be done in a symmetrical order for the structure to remain in equilibrium. Heyman (1982)

Stones in the arch is cut into a trapezoidal shape, voussoir, and joined with mortar, type of stone and mortar used varies vastly. For smaller spans the fit of the stones may not be so cautiously made, instead the stones are joined with a thicker mortar joint. Heyman (1982). The arch can also be made out of bricks joined with mortar, a construction type that is common in the UK. Different shapes of the arch is also possible, e.g. parabolic, segmental or elliptical. The fill over the arch barrel is kept in place by walls, so called spandrel walls. ICE (2008)

An arch bridge is shown in Figure 3.3 were different parts of the arch bridge is explained.

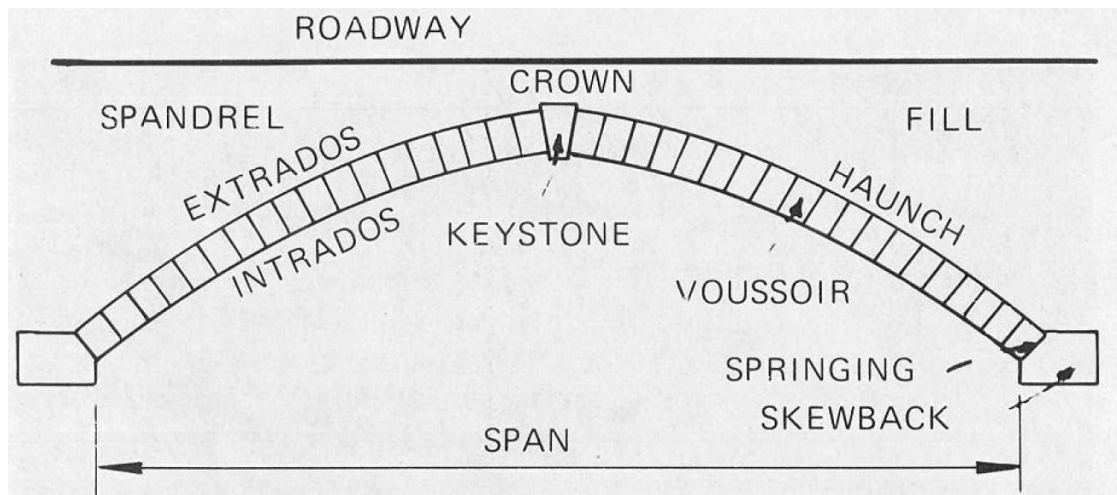


Figure 3.3 Stone arch, explanation of expressions. Heyman (1982)

### 3.2 Arches in history

Although originating from Persians and Sumerians, the historical masterpieces of arch construction were erected by the Romans. The crown of them all is the 270 meter long aqueduct of Pont du Gard in the south of France. The purpose of this construction was to span the river Gard with an aqueduct for a 50 km long water conduit providing water to the city Nîmes. It was constructed 63 -13 B.C. Nationalencyklopedin (2010[1]). River Gard flows 49 meters below the aqueduct and the rise is done in three tiers, Figure 3.4, with the top one containing the water channel. Roman arches were mostly done in a semicircular shape with a span to pier relation of about three to four. The shape of the arches has the advantage that all the voussoirs have the same shape and in Pont du Gard the arches have been constructed without using any mortar. However does the top tier contain mortar for water sealing. Jennings (2004).

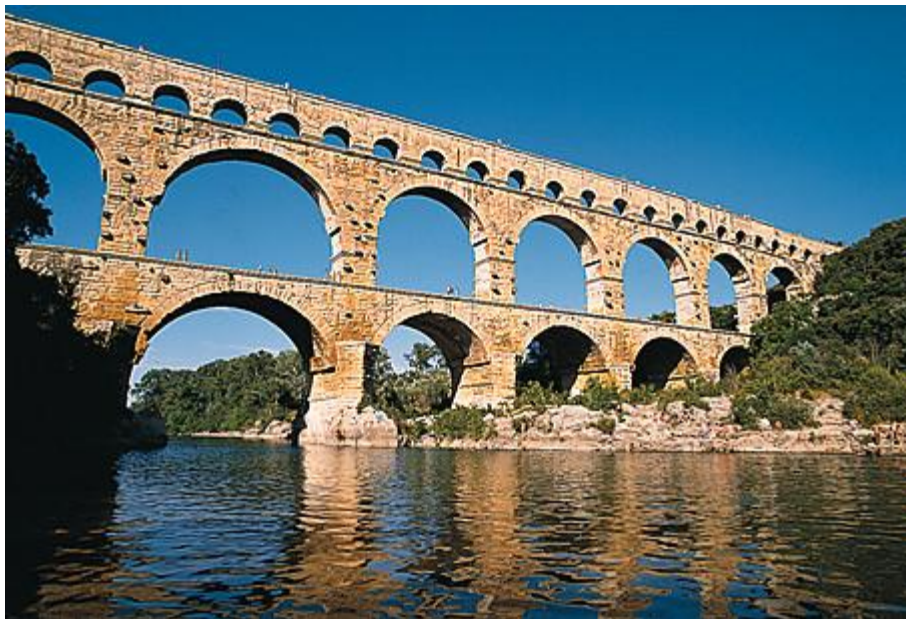


Figure 3.4 The aqueduct Pont du Gard. Nationalencyklopedin (2010[1])

The next step in development of stone arches is the segmental arch bridge. A semi-circular arch have the rise to span relation of 1:2 left in Figure 3.5, while a segmental can have a lower relation like 1:5, right in Figure 3.5. Benefits of this design is larger spans which gives fewer supports and a lower roadway level for a given clearance under the bridge. Jennings (2004)

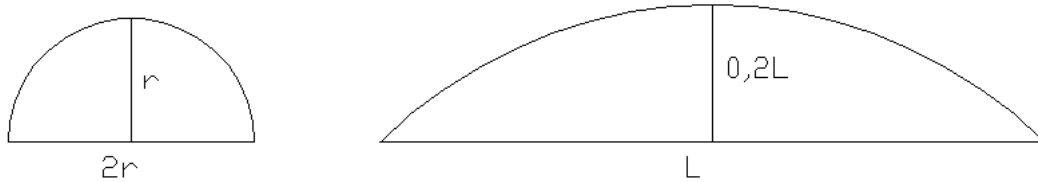


Figure 3.5 Semi-circular and segmental arch shape

In China, the worlds first segmental arch bridge was erected in the seventh century, called the Anji Bridge, Figure 3.6. The rise is 7 m and the span 37 m, giving a span to rise relationship of 1:5,3.



Figure 3.6 Anji Bridge. Wikipedia (2010)

Probably unknowing of this earlier achievement the Italian Taddeo Gaddi designed the segmental arch bridge Ponte Vecchio in Florens, Figure 3.7. A flood had destroyed all bridges leaving an urgent need for a new bridge. Preventing new

flooding disasters the new bridge crossed the river in three spans of about 26 meter, leaving more space for the floodwater. Span to rise ratio were as low as 1:7,5, a record that were unbroken for over 400 years. Jennings (2004).



Figure 3.7 Ponte Vecchio. Nationalencyklopedin (2010[2])

### 3.3 Masonry arch mechanics

The purpose of this thesis work is to show ways of assessing the load carrying capacity. However it may be good for the understanding of the problem that the mechanics of arches are presented.

#### 3.3.1 Assumptions

Two assumptions have to be made before describing the mechanics. These are: The abutments can resist the thrust and that the loads will not lead to crushing of the arch material.

#### 3.3.2 The funicular polygon

“As hangs the flexible line, so but inverted will stand the rigid arch”

This is a quote by the famous scientist Robert Hooke in 1675. It describes the mechanics of arches in a brief, but sharp way. That this is true can be showed using a simple example from Heyman (1982).

A weightless string is subjected to three forces,  $P_1$   $P_2$  and  $P_3$  as shown in Figure 3.8.

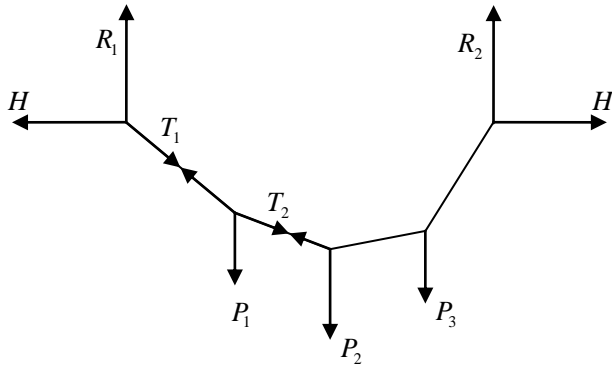


Figure 3.8 A weightless string subjected to three forces.

The inclination of the two first sections of the string is found with the triangles of forces in figure 3.9. These also give the tension in the string. The horizontal force  $H$  is assumed to be known.

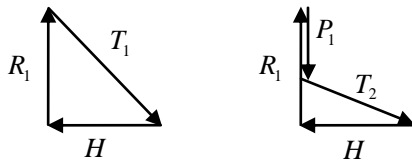


Figure 3.9 Triangle of forces for the string

The triangles can be combined into a complete force polygon, Figure 3.10 below. The reaction forces  $R_1$  and  $R_2$  balances the applied forces  $P_1$   $P_2$  and  $P_3$ . The lines that originate from the top of the  $R_1$  force are the inclinations for the four parts of the string.

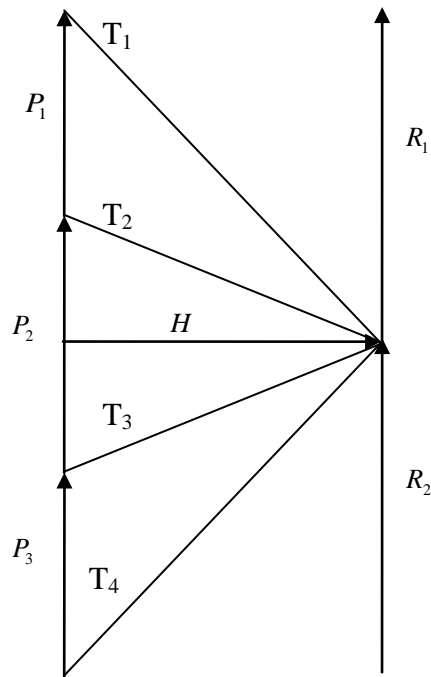


Figure 3.10 The complete force polygon.

To end the string – arch analogy Figure 3.10 can be inverted into Figure 3.11 where the funicular polygon now represents the line of thrust for an arch with the applied forces  $P_1$ ,  $P_2$  and  $P_3$ . Heyman (1982)

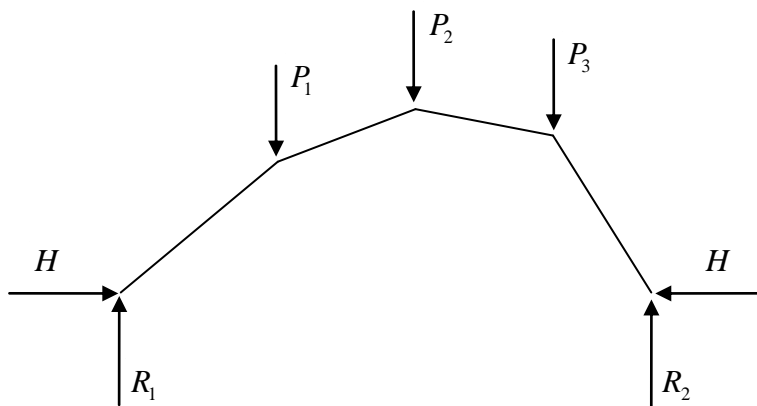


Figure 3.11 The inverted funicular polygon, i.e. the line of thrust for the arch.

### 3.4 The line of thrust

If a new arch is going to be constructed, the designer would have the opportunity to calculate the best geometry for the given loading. The preferred way is to see to that no moments will occur for the so called shape load that the arch is designed for. This means that the line of thrust will coincide with the centre-line of gravity for the arch. Samuelsson A. Wiberg N-E. (1995)

Other loads than the shape load will induce a moment and a transverse force into the arch. This will be the case for masonry arches where there would have been little known about today's loading situation in the design and construction phase. A cut is made to the arch and a system of forces as seen in Figure 3.12 is introduced. Then there is a point at a distance  $e$  from the line of gravity to where all the cross sectional forces can be moved so that the moment is zero. If the arch is cut through at a number of points and the distance  $e$  is calculated for each of them, the line of thrust can be drawn through these points. Samuelsson A. Wiberg N-E. (1995)

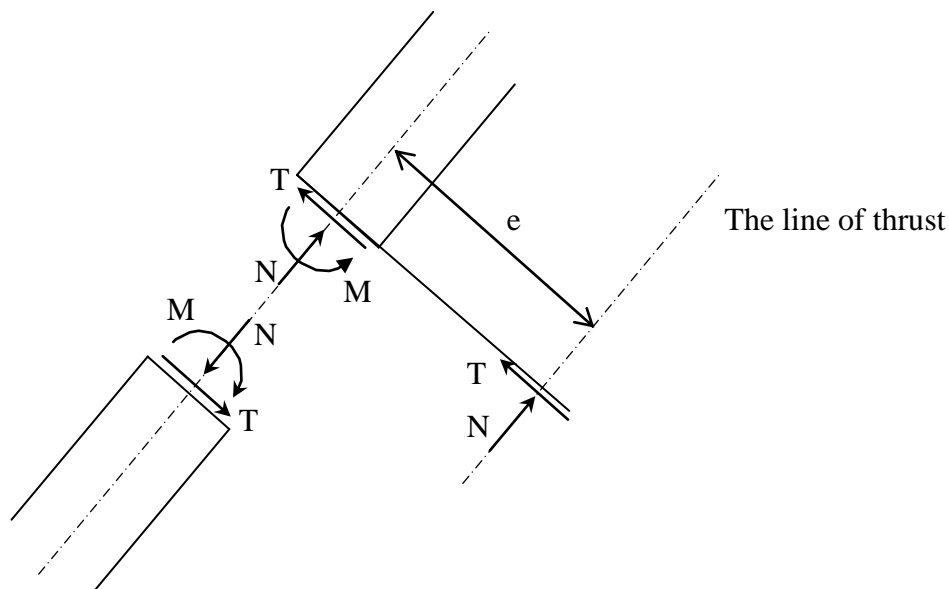


Figure 3.12 A cut through the arch with cross – sectional forces. Reproduced from Samuelsson A. Wiberg N-E. (1995)

Position of the line of thrust has been subject to various design and assessment criterions over the years. The earliest one is “the middle third rule” which is described in section 3.5. More recent methods will be treated in Chapter 4. Sustainable bridges (2007)

### 3.5 The middle third rule

The middle third rule express a limit for the line of thrust to lie within the middle third of the arch thickness. It is based upon elastic theory and the assumption that no tensile

stresses can be transmitted through the mortar material. This can be motivated using an example from Heyman (1982).

Consider a pile of stones that is stacked upon a rigid foundation Figure 3.13(a). If the compressive force, in the arch case the line of thrust, lies in the middle of the pile the stress distribution will be equal over the entire cross section Figure 3.13(b). For a off centre compressive force the stress distribution shifts to a triangular shape, Figure 3.13(c), and when the compressive force reaches the edge of the middle third of the pile, stresses reaches zero at the edge of the pile Figure 3.13(d). Elastic theory gives that when the compressive force have gone passed the middle third the stress distribution should induce tensile force at the right part of the pile, Figure 3.13(e), but the mortar materials inability to resist tensile force gives instead cracking of the arch.

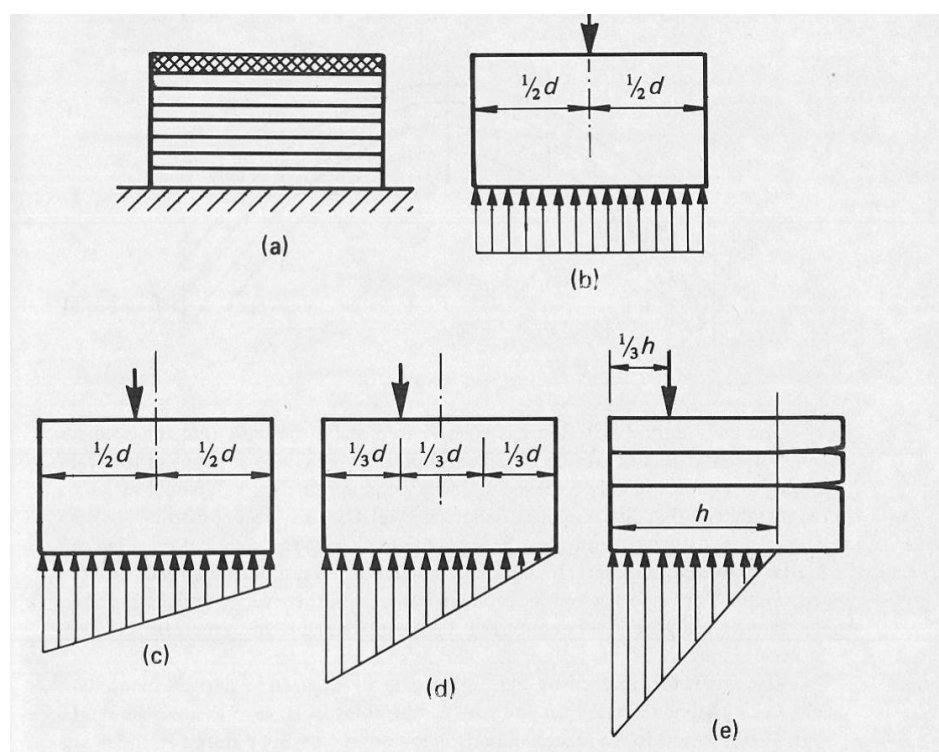


Figure 3.13 A pile of stone subjected to a compressive force. From Heyman (1982).

The middle third rule is very conservative and hard to reach. It requires a good design and heavy dead loads that can offset the live loads. Sustainable bridges (2007)

### 3.6 Pippard's elastic method

As will be seen in Chapter 4.1, the elastic method plays a great role in rough estimation of stone arches. The derivation of that estimations starts with a two pinned arch with horizontal forces keeping the arch in place. A force  $P$  is applied at the top of the arch. The set up can be seen in Figure 3.14. The derivation is reproduced from Heyman (1982) and Sameulsson a. et al. (1995).

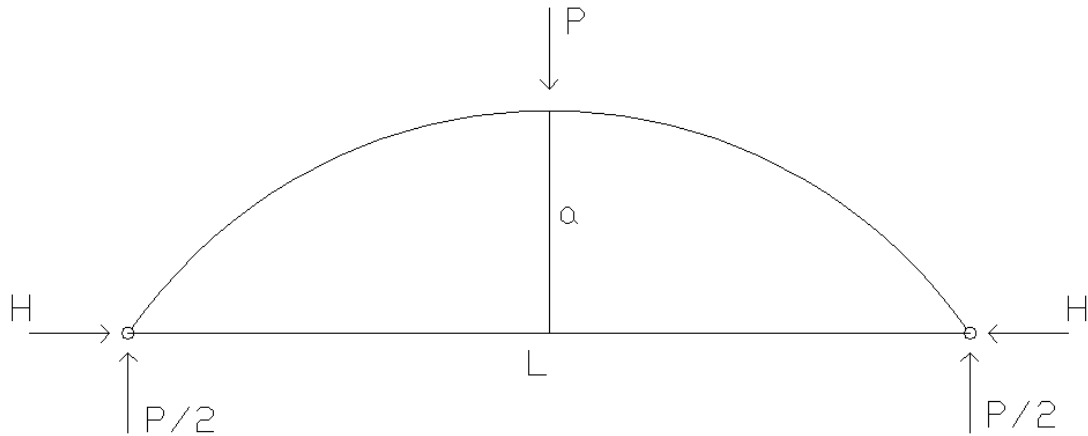


Figure 3.14 Set up for Pippard's elastic method.

The strain energy  $U$  for the arch can be written as equation 3.1, taking into account bending deformations only. Where  $E$  is the Young's modulus and  $I$  the second moment of inertia.

$$U = 2 \int_0^{L/2} \frac{M_x^2}{2EI} ds \quad (3.1)$$

With the use of Menabreas principle (equation 3.2), equation 3.3 is obtained. From equation 3.3 the horizontal force  $H$  can be calculated.

$$\frac{\partial U}{\partial H} = 0 \quad (3.2)$$

$$\frac{\partial U}{\partial H} = \int_0^L \frac{M_x}{EI} \frac{\partial M_x}{\partial H} ds = 0 \quad (3.3)$$

Where  $L$  is the span length and  $ds$  is an arc length.

For simplification, the second moment of inertia of the arch varies like equation 2.3.

$$I = I_0 \frac{ds}{dx} \quad (3.4)$$

Inserting 3.4 into 3.3 gives equation 3.5.

$$\frac{1}{EI_0} \int_0^L M_x \frac{\partial M_x}{\partial H} dx = 0 \quad (3.5)$$

Solving 2.4 gives for the force  $P$ , abutment thrust and crown bending moment as follows.

$$H_p = \frac{25}{128} \frac{L}{a} P \quad (3.6)$$

$$M_p = -\frac{7}{128}PL \quad (3.7)$$

The total thrust and bending moment is a combination of the live load presented above and the dead loads. For the dead loads assumptions are made that the fill and arch have the same unit weight  $\gamma$ , that the bridge width is  $2h$ , the fill height is  $h$  and the arch barrel thickness is  $d$  and that the fill only acts as vertical load on the arch. Strain energy analysis then give in the same way as above values for the dead load abutment thrust and crown bending moment.

$$H_D = \frac{\gamma L^2 h}{a} \left( \frac{a}{21} + \frac{h+d}{4} \right) \quad (3.8)$$

$$M_D = \frac{1}{168} \gamma L^2 ah \quad (3.9)$$

And the thrust parts and bending moment parts can be added respectively.

$$H_p + H_D = \frac{L}{a} \left( \gamma Lh \left( \frac{a}{21} + \frac{h+d}{4} \right) + \frac{25}{128} P \right) = H \quad (3.10)$$

$$M_p + M_D = \frac{1}{4} L \left( \frac{\gamma Lah}{42} - \frac{7}{32} P \right) = M_c \quad (3.11)$$

Considering the highest allowed stress  $f_c$  for the material with the assumption of the arch width as  $2h$  and depth  $d$  using Naviers formula gives equation 3.12.

$$f_c = \frac{H}{2dh} - \frac{3M_c}{hd^2} \quad (3.12)$$

Using the equations 3.10 and 3.11 for thrust and bending moment, the maximum allowed load  $P$  becomes.

$$P = \frac{\frac{256f_c hd}{L} + 128\gamma Lh \left( \frac{a}{28d} - \frac{1}{21} - \frac{h+d}{4a} \right)}{\frac{25}{a} + \frac{42}{d}} \quad (3.13)$$

Small arches have a small cover of fill  $h$  which gives a small width. Two of these small “ribs” can be fitted into a real arch, providing a doubled axle load for a vehicle with a standard track width. See Figure 3.15 for explanation.

$$W = 2P \tag{3.14}$$

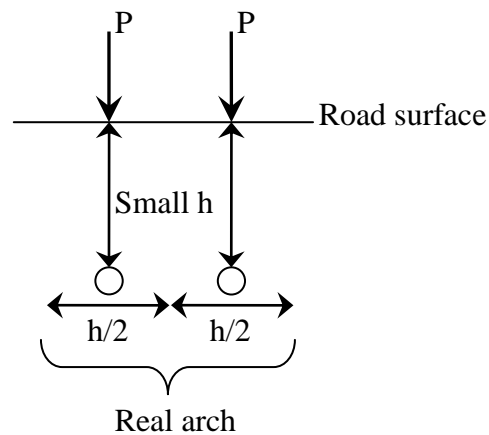


*Figure 3.15 An arch bridge cross section. The two arch ribs can be seen as circles. Because of the small height of the fill the width of one arch becomes small. Then two of these ribs can be fitted into a real arch, raising the allowed axle load to two  $P$ .*

## 4 Methods of calculating load carrying capacity – an overview

There are numerous ways to analyze a stone arch. The development started in World War II and continued during the 20<sup>th</sup> century implementing the old methods and exploring new in computer software. In this chapter a number of the methods are presented. It is not a complete inventory, and not in to deep.

### 4.1 The MEXE method

In Section 2 Pippard's elastic method was presented. Equations 3.13 and 3.14 was in the 1960's combined, for given values of  $\gamma$  and  $f_c$ , into a nomograph, Figure 4.1. This was done by the Military Engineering Experimental Establishment, MEXE, who also gave name to the method. Heyman (1982) For an arch of a certain span and total crown thickness the provisional axle load can be determined by just simply drawing a straight line thru these known points and crossing line C at the provisional axle load for this arch set-up.

To clarify has a dashed line been drawn in the nomograph. The line starts at 7,5 m as span length of the bridge, crossing line B at 0,85 m of fill and arch thickness. This gives, looking at line C, a provisional axle load of 39 tonnes. The MEXE method is limited by the scale shown on line A, B and C and can not be used for other dimensions than these. The highways agency (2001).

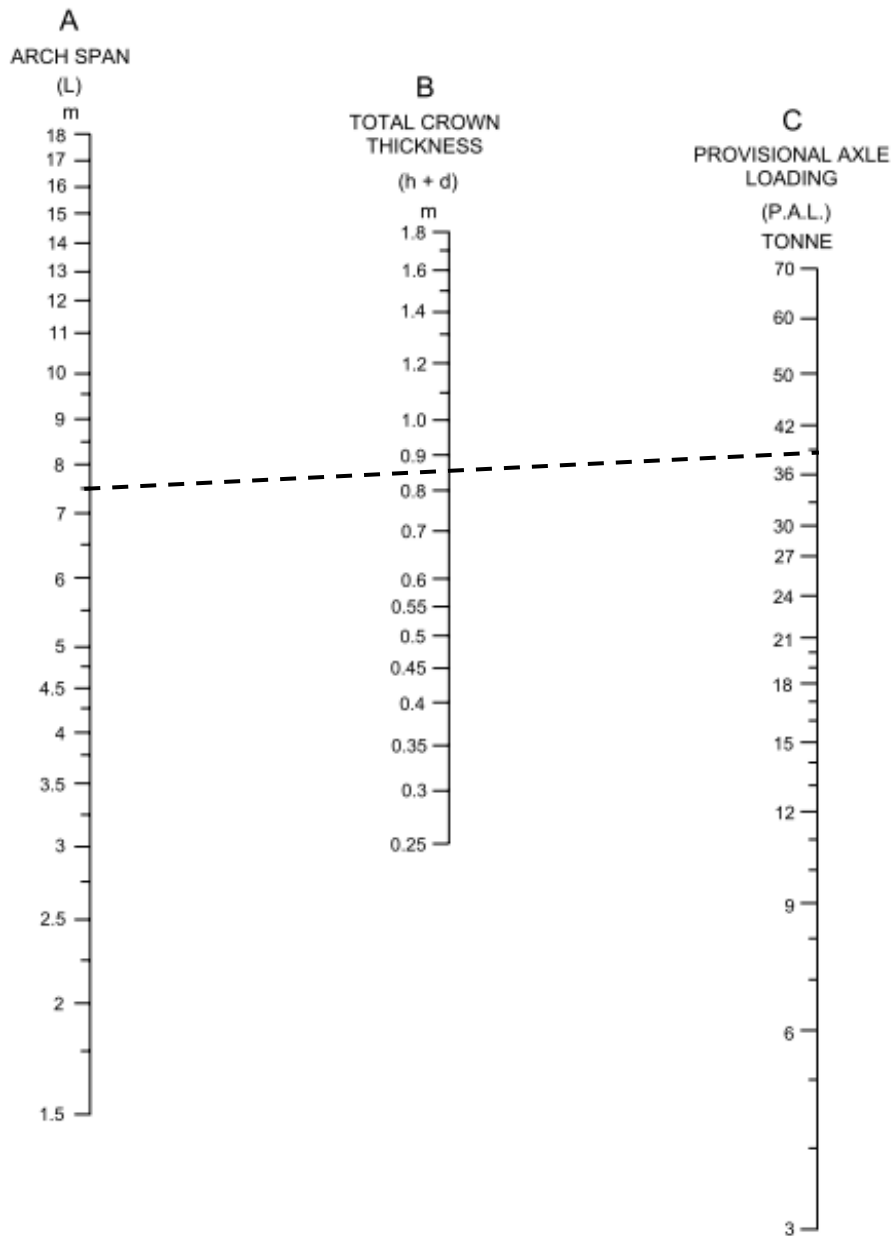


Figure 4.1 Nomograph for determining the provisional axle load. The highways agency (2001).

From the nomograph in Figure 4.1 equation 4.1 has been derived, giving the provisional axle load, PAL. To account for different shape, material, condition etc. of the arch, a number of factors is then used to modify the PAL. The highways agency (2001).

$$PAL = \frac{740(d + h)^2}{L^{1.3}} < 70 \quad (4.1)$$

The modifying factors can be found in both The highways agency (2001) and ICE (2008).

## 4.2 Thrust line analysis

Section 3.5 described the oldest and most conservative version of thrust line analysis, the middle third rule. Another version, but less conservative is the middle half rule. The difference from the middle third rule is, as the name implies that the line of thrust should lie within a section in the middle of the arch with a width of half the cross section, Figure 4.2 shows an arch section with the allowed limit for the thrust line. Sustainable bridges (2007)

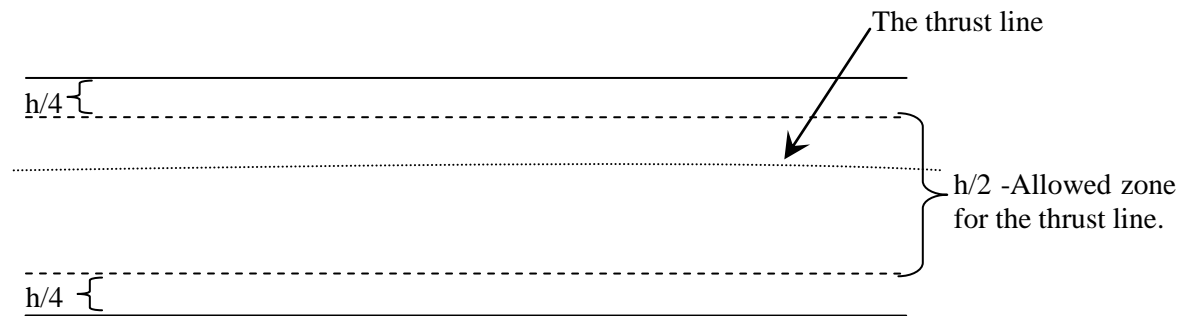


Figure 4.2 Middle half rule.

The least conservative method of thrust line analysis is the mechanism assumption. An arch will be stable even if the thrust line runs outside the arch in three places. But if the thrust line reaches the edge at a fourth place, a mechanism is developed and the structure collapses. An assumption of infinite crushing resistance of the material is needed for this method, something unrealistic in most cases, but for masonry arch bridges stress levels are quite low and this method can therefore be a good method to use. Sustainable bridges (2007)

## 4.3 Thrust zone analysis

A slight modification of the thrust line method is the thrust *zone* method. Now the line of thrust is spread out over a height  $t$  in the cross section, depending on the material compressive strength  $f_c$ , the normal force  $N$  and the thickness  $B$  of the arch. See equation 4.2.

$$t = \frac{N}{f_c B} \quad (4.2)$$

The criterion for the thrust zone method is that the line of thrust should not lie closer to the edge of the arch than  $\frac{t}{2}$ , Figure 4.3. Sustainable bridges (2007)

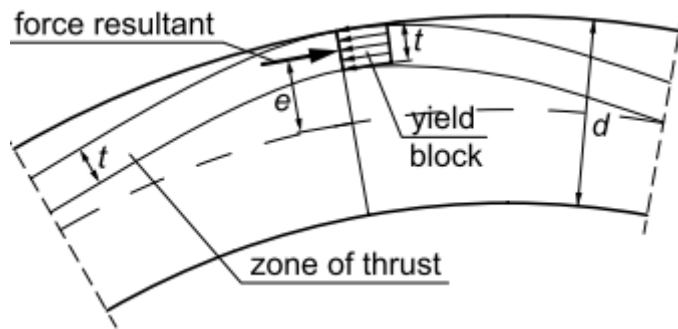


Figure 4.3 The zone of thrust. Sustainable bridges (2007)

## 4.4 Mechanism method

As mentioned in section 4.2 the arch can resist that the thrust line touches the intrados or extrados of the arch at three positions at the same time. When this happens at a fourth location a mechanism develops, leading to arch failure. The scheme of calculation for the mechanism method is as follows. Four places are assumed for hinges on the arch, A, B, C and D. See Figure 4.4.

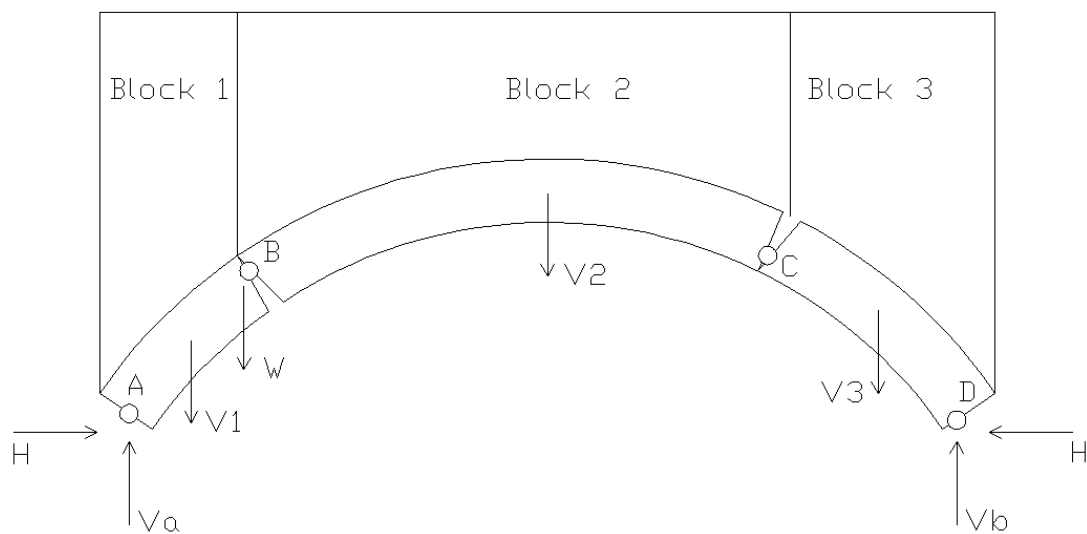


Figure 4.4 Arch with assumed hinges. Reproduced from ICE (2008)

The arch is loaded with a load  $W$  that is applied thru the fill with no dispersion. Self weight from the blocks and corresponding arch segment are denoted  $V_i$ . The system has four unknowns:  $H$ ,  $V_a$ ,  $V_b$  and the collapse load  $W$ . By using moment equations around the hinges, four equilibrium equations can be derived and solved, giving the four unknowns. To get the lowest ultimate load, i.e. the load that is the interesting, the equilibrium equations must be solved for different positions of the hinges. ICE (2008)

## 4.5 Finite Element Methods

FE models of masonry can span from simple one-dimensional bar element joined to a frame, to large work-demanding three dimensional models.

### 4.5.1 Frame analysis

Arches can be idealised as being built up of a number of straight beam elements. The analysis is then conducted using plane frame analysis. Samuelsson A. Wiberg N-E. (1995). The frame analysis is the simplest form of modelling, and the minimum number of straight beam elements that should be used is twelve. ICE (2008). In the analysis the arch is usually considered as fixed at the abutments. Sustainable bridges (2007).

Beam elements that can be used are, in the simplest cases, a two noded beam element with six degrees of freedom, Figure 4.5.



Figure 4.5 Beam element with six degrees of freedom.

#### 4.5.1.1 Tapered beam element

A for masonry adapted version of the beam element is the tapered beam element. When tension occurs in the masonry it cracks and this leads to that the affected region loses its structural stiffness. Also on the compression side, high compression stresses result in crushing of the material and loss of structural stiffness. What is left after cracking and crushing is the effective arch ring which can be divided into tapered beam elements, Figure 4.6. Choo B. S. et al. (1991)

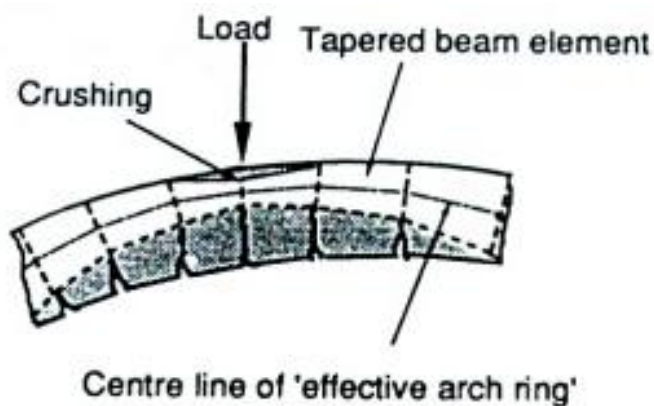


Figure 4.6 Effective arch with tapered beam elements. Choo B. S. et al. (1991).

Crushed and cracked portions of the arch needs to be removed in the analysis considering smaller area and a reduced second moment of inertia.

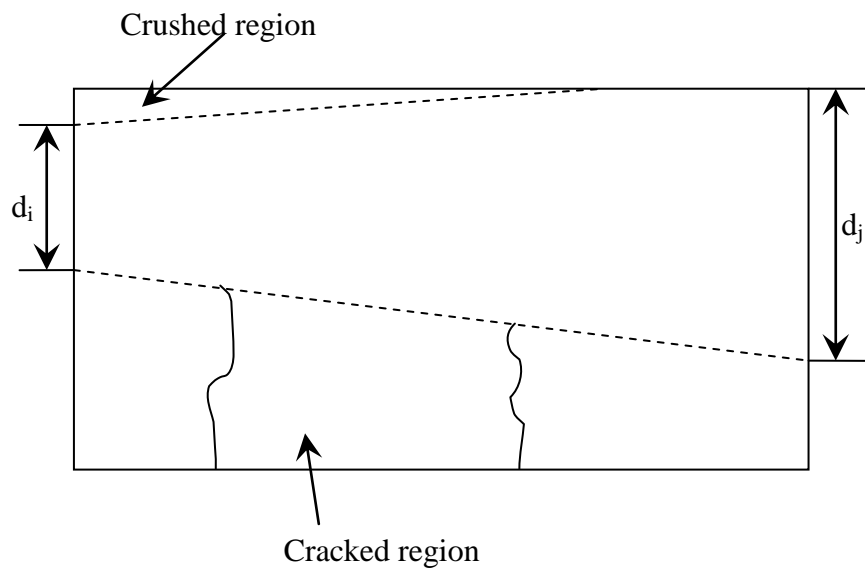


Figure 4.7 The tapered beam element with crushed and cracked zones.

The area and second moment of inertia for the element is computed with equation 4.3 and 4.4, compare with Figure 4.7. These are then inserted into the element stiffness matrix for tapered beam element.

$$I(x) = I_i + \frac{(I_j - I_i)x}{L} \quad (4.3)$$

$$A = \frac{(A_i + A_j)}{2} \quad (4.4)$$

The different depths  $d_i$  and  $d_j$  are computed by equilibrium equations, see further Choo B. S. et al. (1991).

#### 4.5.2 Two and three dimensional FEM

Masonry can also be modelled in two and three dimensions. An example of the two dimensional case is seen in figure 4.8.

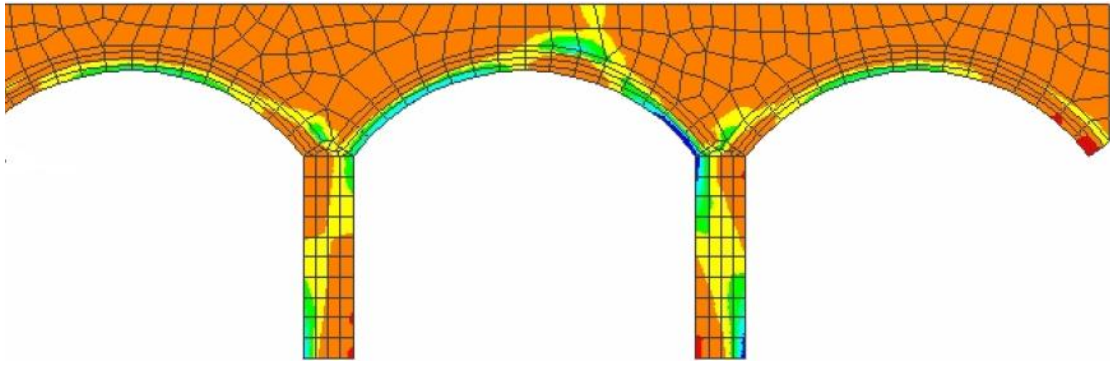


Figure 4.8 A masonry arch bridge modelled in 2D FEM. Sustainable bridges (2007).

The three dimensional models of masonry are work demanding but have the benefit of possibility to model the entire structure like spandrel walls and abutment wings. Including these parts to the simulation may grant a better result of load carrying capacity. Sustainable bridges (2007)

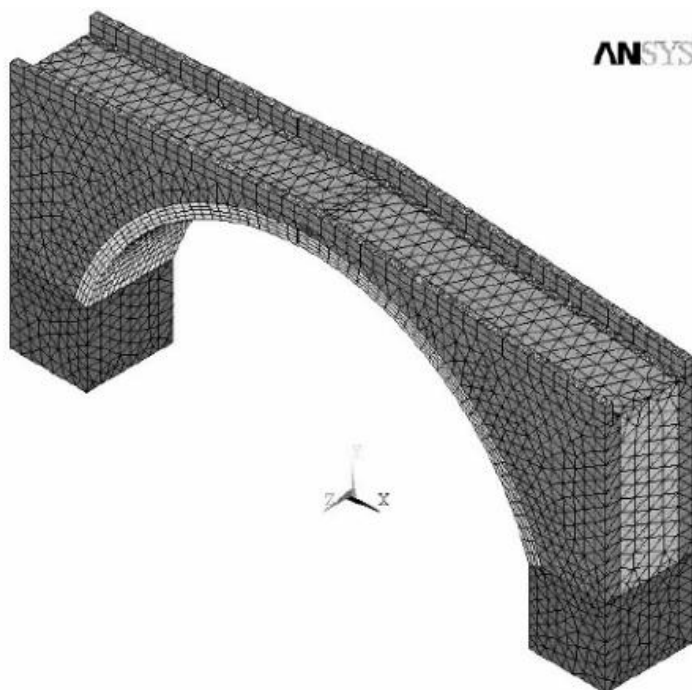


Figure 4.9 A masonry arch bridge modelled in 3D FEM (ANSYS). Sustainable bridges (2007).

## 4.6 Discrete Element Method

The Discrete Element Method, or DEM, is a computational technique where the structural parts usually are modelled as 2D blocks but can also be in 3D. These blocks, that can be rigid or deformable, are able to move and interact with each other.

The behaviour of the blocks is obtained by solving the dynamic equations of equilibrium for the interaction between the blocks. Sustainable bridges (2007)

Benefits with DEM methods are the possibilities of modelling loose stones that fall out of the arch, and that stones can have new interaction points if the arch is deformed. This is only possible to achieve in “high end” FEM software that needs powerful computing. Tóth A. R. et al. (2009)

There are two common discrete element methods used for masonry arches, UDEC (Universal Discrete Element Code) and DDA. From the beginning UDEC was used to make models of rock, but it has developed into a commercial DEM program. Blocks in the program can be modelled either as rigid or deformable blocks. The deformable blocks are divided into finite uniform-strain elements. Displacements are calculated during a finite time step using Newton’s force-acceleration law, using explicit time integration based on central differences. A UDEC model of an arch is seen in Figure 4.10. Tóth A. R. et al. (2009)

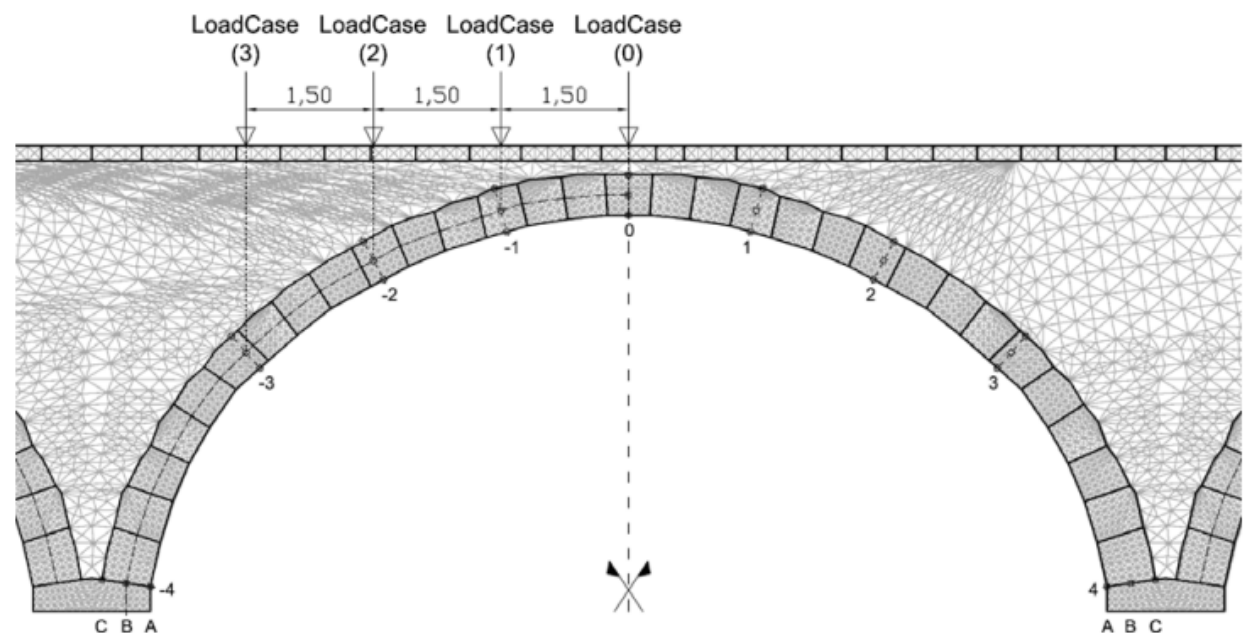


Figure 4.10 A masonry arch modelled in UDEC. Tóth A. R. et al. (2009)

Discontinuous Deformation Analysis, DDA, is the other version of discrete element method. In this method, every element is given a reference point which then can translate, and around the reference point the element can rotate. DDA considers the contacts between the elements and the forces they act upon each other and also the stiffness matrix of the system. The time stepping scheme used is the Newmark- $\beta$  method. Tóth A. R. et al. (2009)

There is also a three dimensional version of UDEC, called 3DEC. An example of a masonry arch modelled in 3DEC is shown in Figure 4.11.

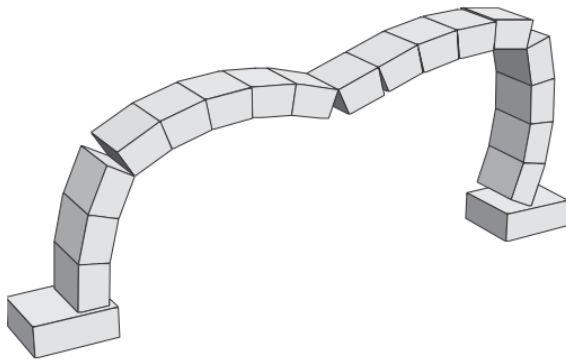


Figure 4.11 A masonry arch modelled in 3DEC. Lemos J. V. (2004)

## 4.7 Commercial software: RING2.0

RING 2.0 is based upon the mechanism method to analyse the ultimate state, i.e the maximum load that can be applied on the arch. The program does not use the trial and error mechanism procedure presented in Section 4.4 to find the critical load case, but instead mathematical optimization technique. It also takes (if selected) the arch materials compressive strength into account as a thrust zone, see Figure 4.12. Backfill acts restraint when the arch moves into the backfill, the activated backfill elements are shown as blue bars, Figure 4.12. It is also possible to model the bridge as a railway bridge with tracks and sleepers instead. LimitState (2009)

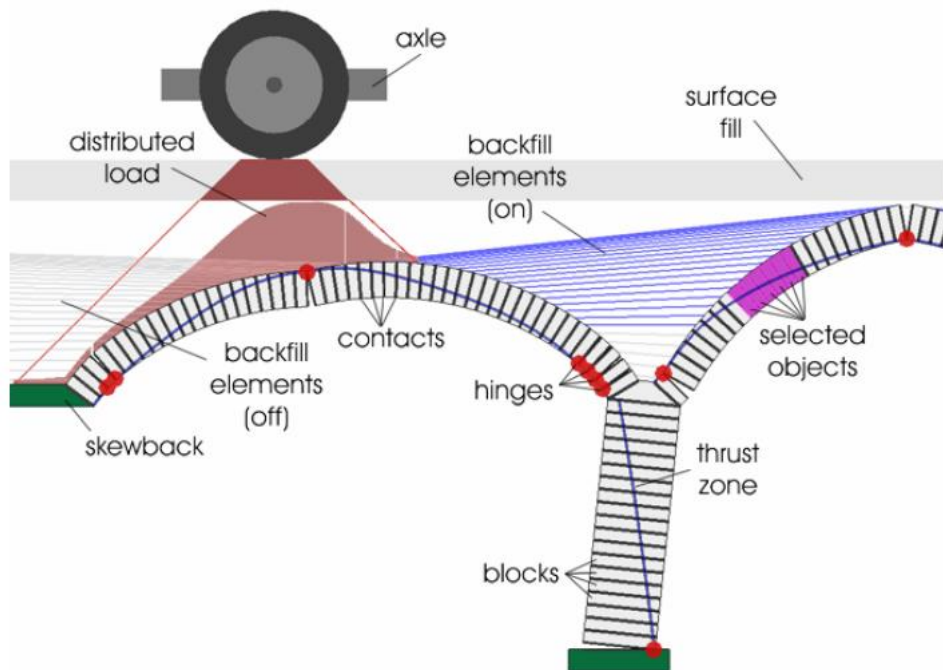


Figure 4.12 A screenshot from a RING2.0 analysis with explanations. LimitState (2009)

## 4.8 Commercial software: Archie-M

Archie-M uses the thrust zone analysis described in Section 4.2 for the analysis. The program can handle multi-span arch bridges and considers the backfill as a continuous mass. The backfill disperse the load onto the arch and provides both active and passive soil pressure. Sustainable bridges (2007)

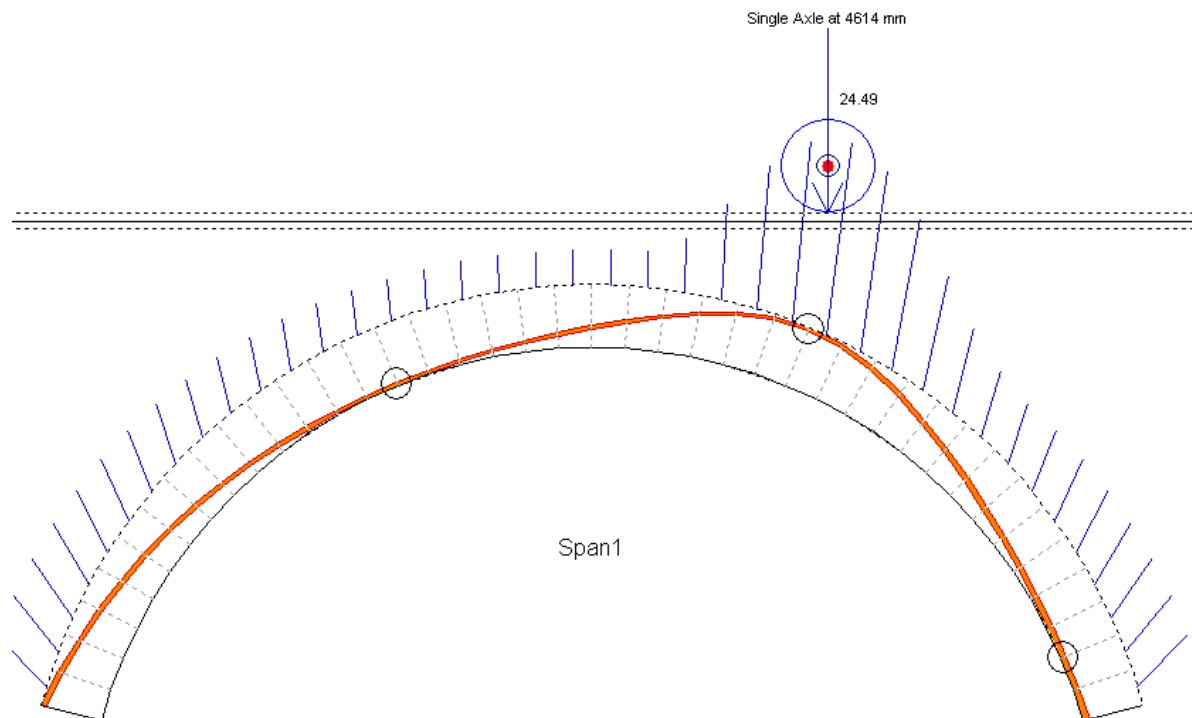


Figure 4.13 A masonry arch modelled in Archie-M.

Figure 4.13 shows a screenshot from an analysis carried out in Archie-M. The three circles are the most likely hinges of a three pinned arch for the given loading. As long as the zone of thrust, the orange line, is within the boundaries of the arch it is in equilibrium, when the zone of thrust reaches the boundary at a fourth place, ultimate state is reached.

Also Archie-M give the possibility to model the bridge as a railway bridge.

## **5 Comparison of different calculation methods – literature survey**

The aim of this thesis is to compare and try to evaluate different calculation methods for assessing stone and masonry arch bridges. The evaluation part is quite difficult because the lack of known parameters and possibilities to compare one arch with another. Programs and methods can be compared with each other for example regarding what deflections and ultimate load they show for a certain arch. But the correlations with reality for these results are harder to say anything about. However there have been full scale tests done in the U.K by the TRL (Transport Research Laboratory) where masonry arch bridges have been loaded to failure.

There have been a number of comparisons made where different methods have been used on the same arch to see what differences they give in the ultimate load capacity. This chapter is aimed to give an overview over these studies and also the studies where computational methods have been compared to real tests. It will also be shown that it is possible to achieve good results with computational techniques.

### **5.1 Test results**

In the eighties the UK:s Transport Research Laboratory, TRL, (formerly TRRL) loaded a number of decommissioned masonry arch bridges to failure. Five bridges are presented in Crisfield M. A. et al. (1987), but other bridges appear in the literature. The five bridges in Crisfield M. A. et al. (1987) are: Bargeower, Bridgemill, Preston, Prestwood and Torksey. The first three were made of stone voussoirs and the last two of brick. In Sweden there are not any brick bridges so these will be left out from comparison.

### **5.2 Computations compared with tests**

Because of the lack of full scale tests except for the above mentioned, these have to serve as some kind of benchmark for computation methods. However there have been some laboratory tests of masonry arches that will be presented.

#### **5.2.1 The MEXE method**

Results from the MEXE method are quite much up to the engineer's discretion and judgement. How the ultimate load presented in Table 5.1 is calculated in terms of factors is unknown, but it shows a dramatic gap between experimental and calculated loads. An explanation of the gap is that MEXE is a serviceability calculation more than a ultimate load calculation. Crisfield M. A. et al. (1987).

Anyway, a conclusion based on the presented data is that the MEXE method is conservative and that it can be a good idea to use some other method to calculate the load carrying capacity.

Table 5.1 Comparison of the MEXE method and experiments. Crisfiled M. A. et al. (1987)

	Bargeower	Bridgemill	Preston
Experimental collapse load (kN)	5600	3100	2100
MEXE method (kN)	1285	363	597

### 5.2.2 FEM using tapered beam element

Choo B .S. et al. (1991) have used the tapered beam element to analyse the Bridgemill, Bargeower and Preston bridges. Material parameters used in the model are based on the tests that were done on the materials from the tested bridges. Results from these tests are scanty and estimates of parameters have been used where information have been missing. Result for one bridge is shown in Figure 5.1 and it shows a very good agreement in both load – deflection relation and collapse load for the Bargeower Bridge.

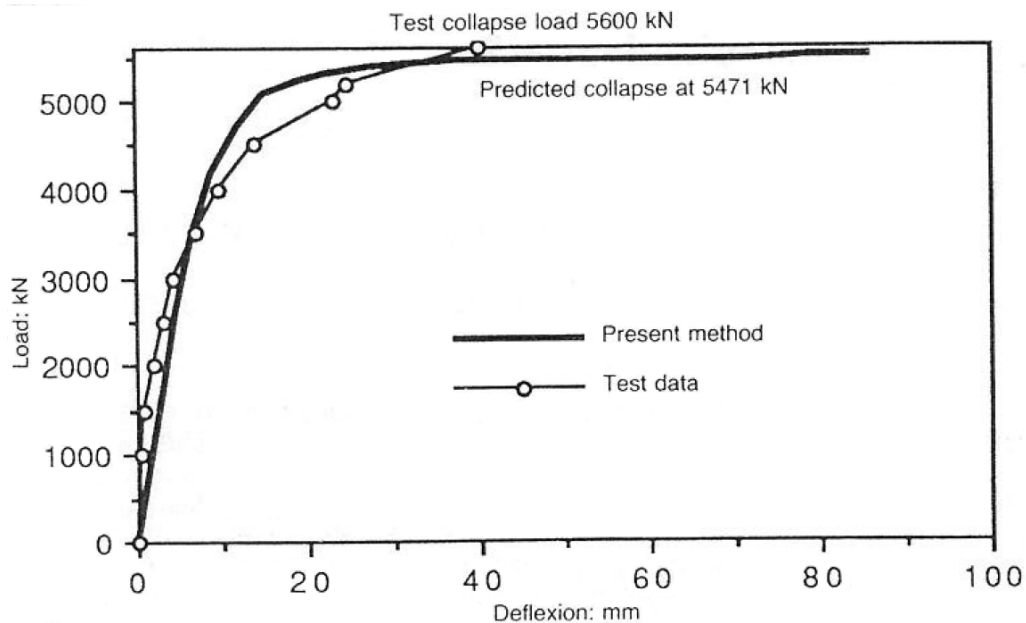


Figure 5.1 Load – deflection relation for Bargeower Bridge for both experiment and tapered beam analysis. Choo B. S. et al. (1991)

### 5.2.3 3D FEM – ABAQUS

Berndtsson et al. (1999) modelled the Barlae Bridge which were part of the research study where decommissioned masonry bridges were loaded to failure. The bridge was

within the 1999 study modelled in Abaqus and after various attempts the failure load in the simulation was 2750 kN. In the full scale test the failure load was 2900 kN, or 5,5 percent deviation.

## 5.2.4 RING

The manufacturer of RING, LimitState presents results from a TRL report from 2001 on the subject of RING compared with the results from the full scale tests. This report has not been possible to retrieve for this thesis but it is presented using LimitState (2009).

Table 5.1 shows the percentage of theoretical collapse load relative to the experimental ultimate load. The version of RING used for this comparison was 1.1 and 2.0 which is the one used in chapter six. What parameters that have been used for backfill etc. is unknown and LimitState (2009) implies that there have been some lack of parameters for modelling. Considering this, good results have been obtained in comparison with the full scale tests, Table 5.1.

*Table 5.1 Comparison of RING computational results and experimental results. LimitState (2009)*

<b>Bridge</b>	<b>Theoretical/experimental load</b>
Bridgemill	100%
Preston	90%
Barlae	92%

Results from RING2.0 have also been compared to test done at the University of Salford in order to study arch-soil interaction. Table 5.2 shows the results from the test and also two simulations done in RING2.0, one for default values in the program (except backfill unit weight) and one with measured properties. The span of the two bridges was 3 meters and they were built in a housing filled with soil. LimitState (2009)

Table 5.2 Comparison of RING and experimental results. LimitState (2009)

Bridge	Description	Experimental collapse load (kN)	ring2.0 analysis		ring2.0 (B) / experiment
			(A) Default soil properties except using measured unit weight	(B) As (A) but also using measured soil strength properties	
1	3m single span - limestone fill	126	84	120	95%
2	3m single span - clay fill	92	88	90	98%

### 5.2.5 UDEC

No information has been found about UDEC and comparison with the above mentioned full scale tests. However there has been a comparison made with a laboratory built replica of a cloister façade. The test set-up is shown in Figure 5.4.

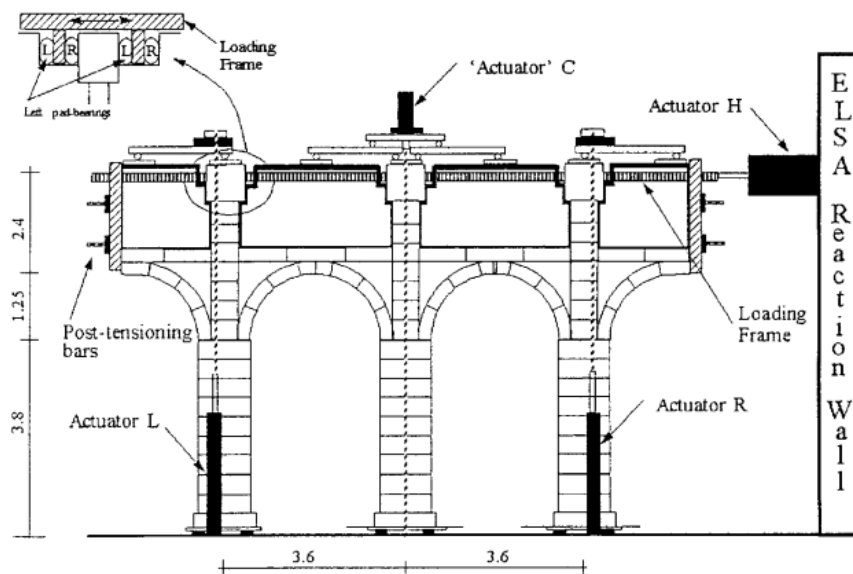


Figure 5.4 Test set-up of a historical masonry façade. Giordano A. et al. (2002)

The analysis in UDEC have been done using a desired displacement history and from that obtaining the force displacement relation shown in Figure 5.5. Giordano A. et al. (2004).

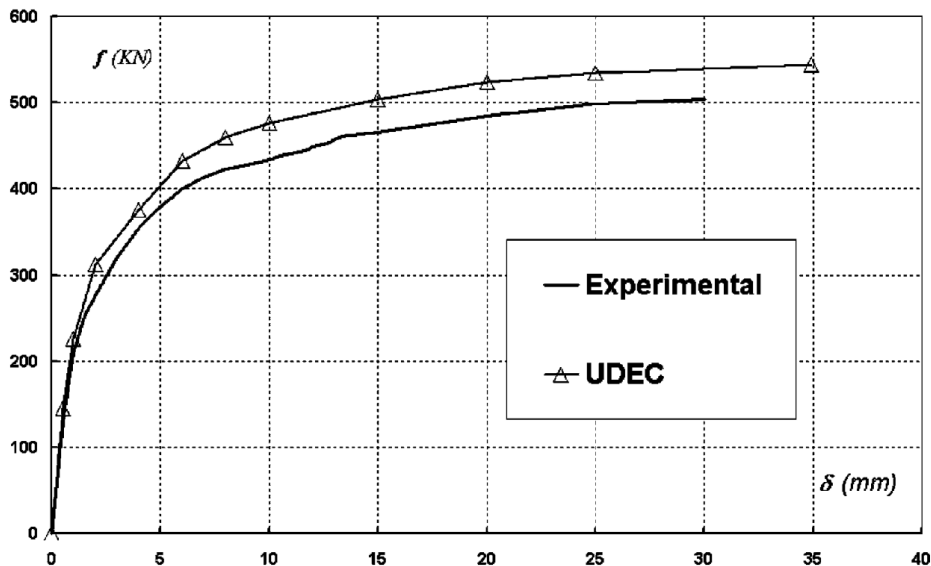


Figure 5.5 Results from experiment and UDEC simulation. Giordano A. et al. (2002)

As seen, the experimental curve and computational curve follow each other quite well, but the maximum load is overestimated. The authors say that this “may be connected with simple modelling of the masonry infill”. Giordano A. et al. (2004)

### 5.3 Comparison of computational methods

#### 5.3.1 FEM, RING and Archie-M

A EU project called Sustainable bridges (2007) have done comparative calculations of a 5 m span arch bridge with two different rise/span ratios. Thickness of the arch barrel was 45 cm and fill height over arch crown was 35 cm. A single axle was positioned over the quarter point of the span and the ultimate load was then calculated. Compared methods were two dimensional FEM, RING and Archie-M. Please observe that the RING version used for this survey is an older version than RING 2.0 that is presented in this report. Results from the comparison are shown in Table 5.2.

Table 5.2 Maximum single axle load at quarter point of span, in kN. Reproduced from Sustainable bridges (2007)

Rise/span	FEM	RING	Archie-M
1/2	424	412	445
1/4	435	459	440

Results from all three methods are in quite close proximity to each other with a maximum deviation of 8 percent.

### 5.3.2 UDEC and RING2.0

Tóth A. R. et al. (2009) presents a study where a multispan masonry arch bridge has been modelled in UDEC, see chapter 4.6, and a comparison was made with RING2.0. Figure 5.6 shows the correlation between UDEC and RING2.0 for different backfill materials regarding the load carrying capacity of span 3 of the multi span bridge. It can be mentioned that the UDEC model has evolved from a single span in situ test of a real arch where the difference between measured and calculated deformation only is 0.004 mm. Tóth A. R et al. (2009)

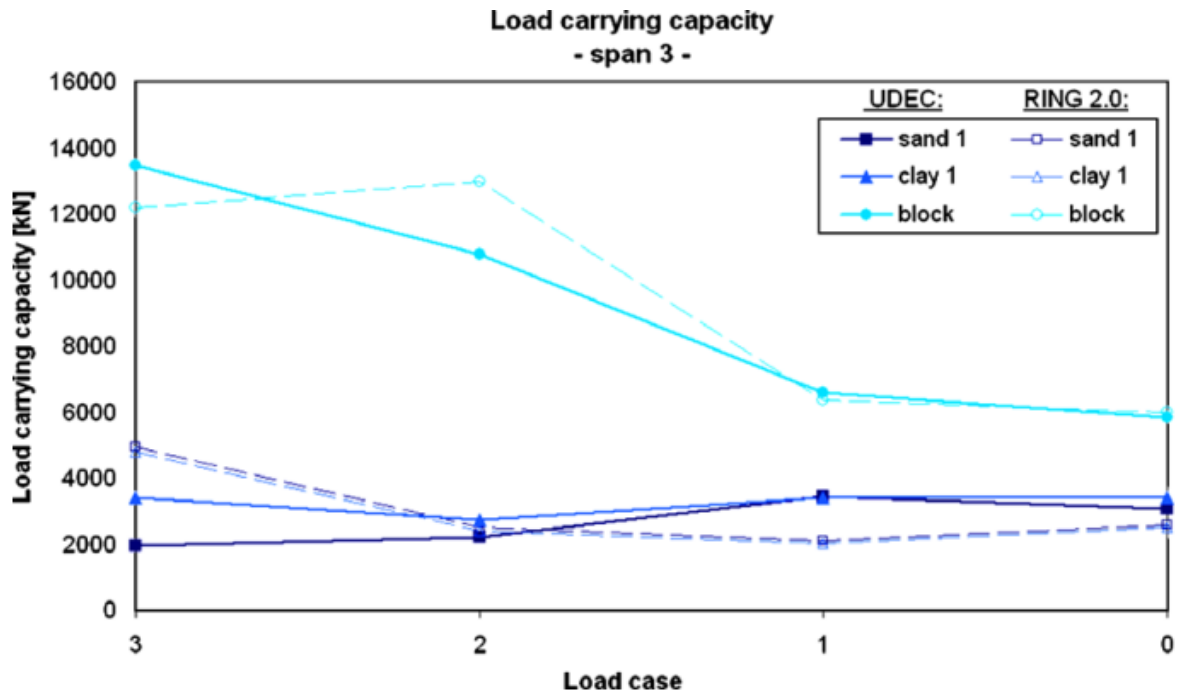


Figure 5.6 Comparison of RING2.0 and UDEC regarding load capacity of a multi span bridge. Tóth A. R. et al. (2009)

It can be seen that there are rather good correlations between the results from both programs for all three backfill materials.

### 5.3.3 ANSYS and 3DEC

Schlegel R. et al. (2004) have analysed the difference in ultimate loading for a continuum modelled arch in ANSYS and a discrete model in 3DEC. Arch and spandrel walls are prescribed with material parameters for historical sandstone. Spandrel walls are modelled with weaker masonry than the arch barrel and the arch has no backfill. One continuum model was analyzed in ANSYS and two discontinuum models with to different stone sizes in the spandrel walls. One model called 1x0,5 and a model with twice the stone size called 2x1. Failure plots from both programs are shown in Figure 5.7 and Figure 5.8.

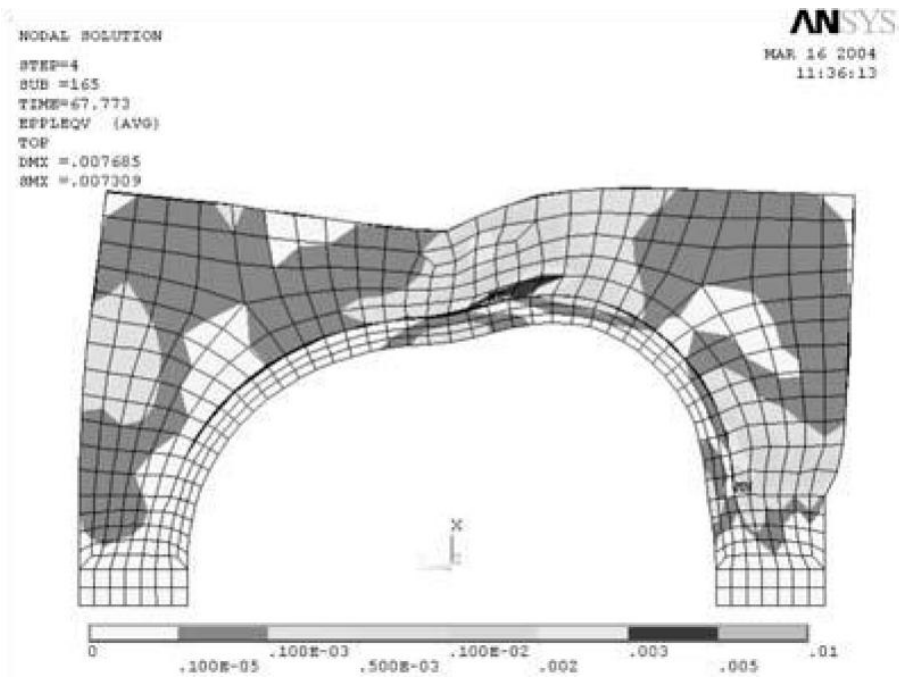


Figure 5.7 Plastic strains in the arch when ultimate load is applied in ANSYS. Schlegel R. et al. (2004)

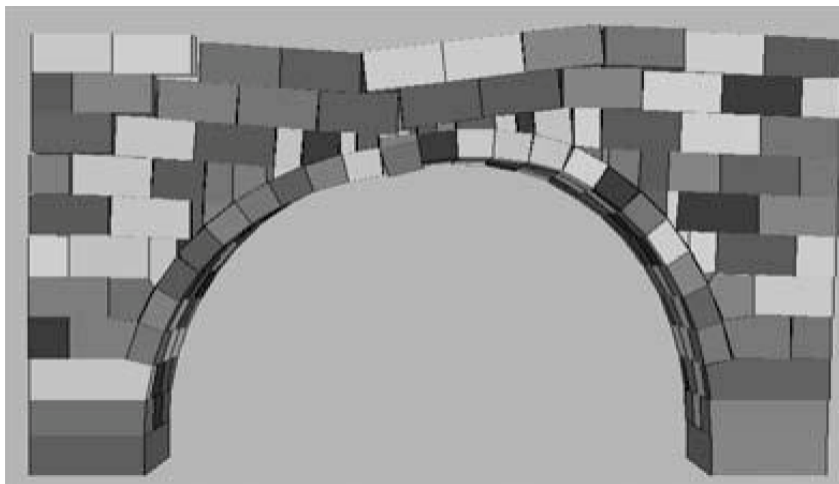


Figure 5.8 Failure mechanism in 3DEC. Schlegel R. et al. (2004)

## **6 Parametric study – influence of different material parameters on the load carrying capacity**

The previous chapter showed that it is possible to model masonry accurate. What it also showed is that the material parameters are crucial to obtain a good result. Therefore will a parameter survey be done in the following chapter to see what influence different material parameters have on the load capacity. Results from this survey are interesting for the sake of inspections and which parameters that should be determined when assessing stone arch bridges.

During the parametric study the geometry of the arch will be fixed while material parameters will be changed. The parameters that affect the capacity the most are also the most important to study in an inspection.

### **6.1 Material parameters**

Before starting the parametric study the set and range of parameters that should be varied must be determined.

#### **6.1.1 Arch barrel**

Compressive strength and density of the arch barrel material are the material parameters that are changeable for the barrel, except for the coefficient of friction between the block and masonry. This parameter is prescribed in the regulating design code, see Table 3.1, and will be left unchanged during the parametric study.

Swedish conditions mean granite in the major part of the stone construction. So the material parameters for arch barrel need to be based on characteristics for granite masonry. Figure 6.1 show characteristic strength for different masonry compositions. Most interesting is the ashlar line under the granite arrow showing a characteristic strength of about  $17 \text{ N/mm}^2$ . ICE (2009).

Ashlar is fine cut rectangular stones that are used for building. Nationalencyklopedin (2010[3]). An arch made out of voussour may be considered as an ashlar masonry structure.

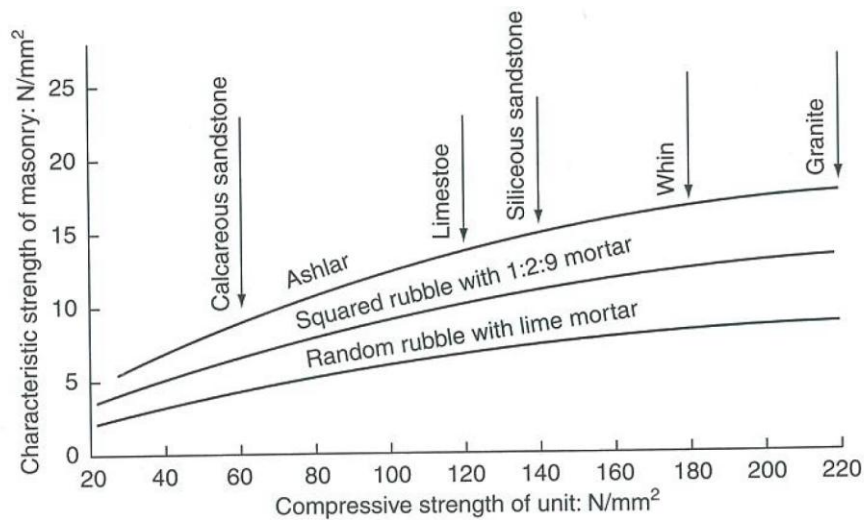


Figure 6.1 Characteristic strength for different types of masonry. ICE (2009)

Material testing of granite masonry has been done by Vasconcelos G. et al. (2009) to evaluate the compressive strength. Tests were conducted both with fine cut stones without mortar, rough stones without mortar, stones with lime mortar and stones with soil mortar. The test set-up for the specimen with soil mortar is shown in Figure 6.2.



Figure 6.2 Test of compressive strength for granite prisms joined with soil mortar. Vasconcelos G. et al. (2009)

Results of tests for both the compressive strength and modulus of elasticity are shown in Table 6.1.

Table 6.1 Material properties for different granite-mortar compositions. Vasconcelos G. et al. (2009)

	Compressive strength [N/mm <sup>2</sup> ]	Modulus of elasticity (E <sub>c</sub> ) [N/mm <sup>2</sup> ]
Fine cut without mortar	73,0	14722
Rough cut without mortar	51,9	7934
Lime mortar	37,0	4629
Soil mortar	64,2	8920

These results show much higher values than is proposed in ICE (2009). A good range for the compressive strength is suggested to be 15 N/mm<sup>2</sup> to 45 N/mm<sup>2</sup>.

The density of granite varies between about 2.5 to 2.8 g/cm<sup>3</sup> (~ 25 – 28 kN/m<sup>3</sup>), see Figure 6.3. Encyclopaedia Britannica (2010). The interval also includes the unit weight of stone masonry of 27 kN/m<sup>3</sup> presented by The Swedish Rail administration. Banverket (2005)

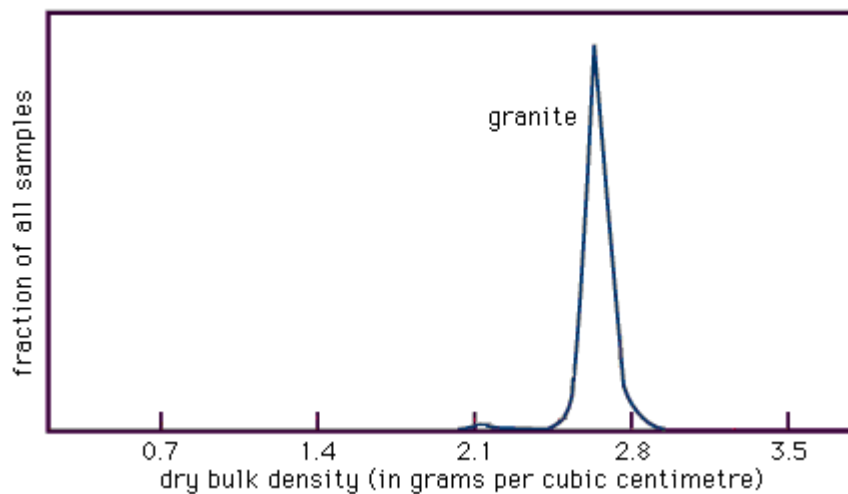


Figure 6.3 Density of granite. Reproduced and edited from Encyclopaedia Britannica (2010)

## 6.1.2 Backfill

The material parameters of the backfill that will be varied is the density, cohesion and angle of friction. The angle of friction and cohesion can't vary independently to each other but will be described in pairs. On top of this the height of the fill will be varied.

Backfill can be assumed to consist of anything from clay to ballast. This needs to be decided during inspection, but for the parametric study different combinations of backfill will be tested to see the impact on the load capacity.

### 6.1.2.1 Weight

The weight of possible backfill materials doesn't vary vastly. Table 6.2 presents weights of these materials when they are above ground water and contains natural moisture. Vägverket (2010[1])

Table 6.2 Weight of backfill materials. Vägverket (2010[1])

Material	Weight [kN/m <sup>3</sup> ]
Clay	17
Sand	18
Gravel	19
Coarse crushed stone	20
Reinforcement layer material	22

In the parametric study weight of the material will be changed between 17 and 22 kN/m<sup>3</sup> based on Table 6.2.

### 6.1.2.2 Angle of friction and cohesion

As said does not the angle of friction and cohesion vary totally independently. A frictional soil with large particles like gravel has no cohesion. A more fine coarse soil can have both frictional angle and cohesion. The angle of friction is a measure of the mechanical strength of the material, and the cohesion is a measure of the adhesive forces between the particles that the soil consists of. Swedgeo (2010)

Table 6.3 shows the angle of friction for some frictional materials without cohesion. The values are for dense materials. Because of previous traffic on the bridge the backfill material may be considered as dense.

Table 6.3 Angle of friction for backfill materials. Vägverket (2010[1])

Material	Angle of friction [deg.]
Silt	33
Sand	35
Gravel	37
Sandy moraine	42
Ballast	45

In the parametric study the angle of friction will be varied between 33 and 45 degrees with no cohesion present.

For the backfill materials with cohesion there are no clear values for the cohesive forces. The frictional angle for clay is 30 degrees, Vägverket (2010). Cohesion varies between 10 and 100 kN/m<sup>2</sup> in the survey made by Tóth A. R. et al. (2009), those parameter values will be used also in this report.

### 6.1.3 Arch geometries

Two different arch geometries will be used for the parametric study. Both of them are geometries from actual arches. The first of them is an arched culvert under an industrial plant. The stream that flows thru it is called Visman, so further on this arch will be referred to as the “Visman arch”. Dimensions for the arch can be found in a cut out from the original drawing, see Figure 6.4

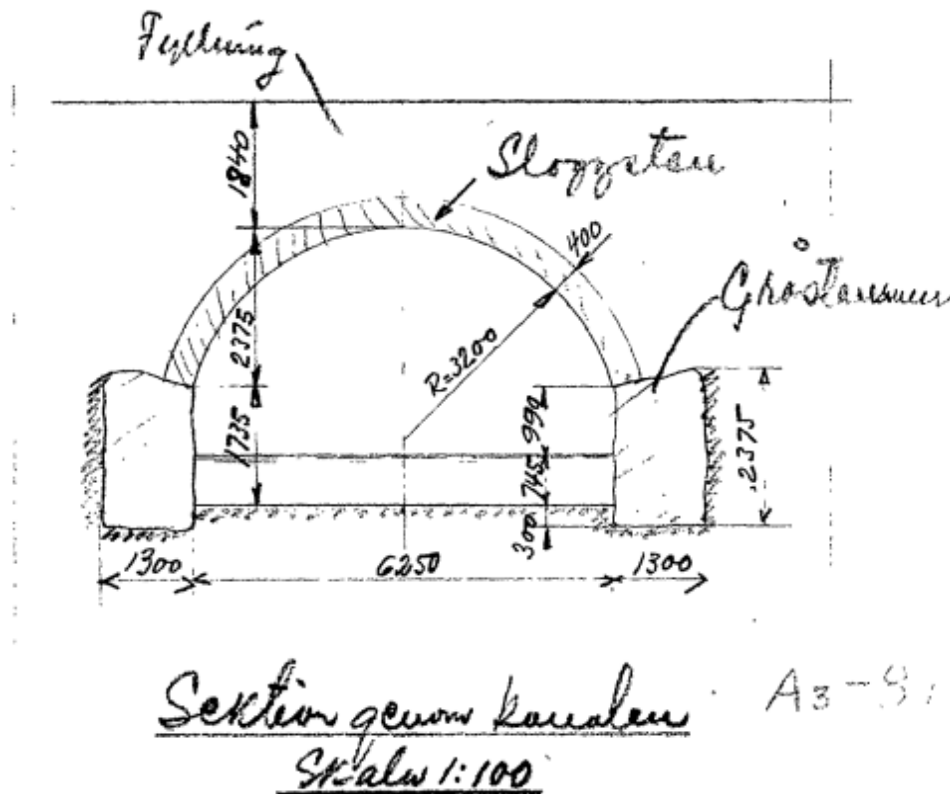


Figure 6.4 Original drawing of the arch.

The old drawing suggests that the span is 6,250 m and measurement on site show that this is close to reality. There is some geometrical inconsistency for the dimensions given in the original drawing considering the span/radius/rise relationship. A revised

drawing can be seen in Figure 6.5 keeping the rise as fixed and adjusting the other dimensions.

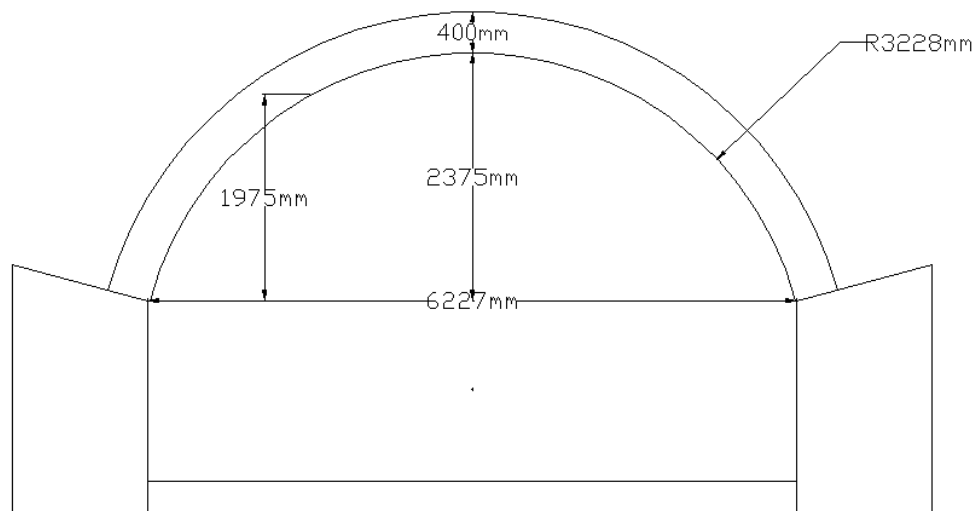


Figure 6.5 Revised drawing of the arch.

The second arch is the previously mentioned Bridgemill bridge that was tested in the full scale tests done by TRL. The span of this bridge is almost three times the span of the first bridge in this parametric study. Figure 6.6 shows the full geometry of the arch. The measures is obtained from Crisfield (1987)

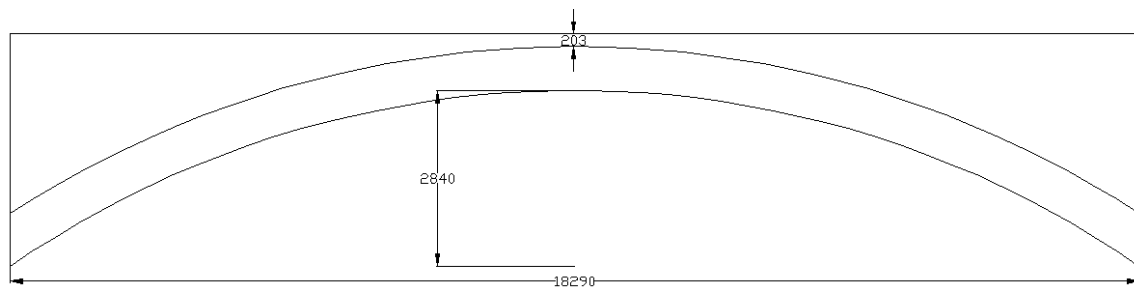


Figure 6.6 Bridgemill bridge geometry.

From these arches only the geometry will be taken. They have very different shapes and spans making them interesting to compare. Things like abutments etc. is not taken from the two arches.

The width of the arches that is used for the parametric survey is 2,5 m.

#### 6.1.4 Loading

For the parametric study a double bogie load will be used with a distance between the axles of 1 m and track width of 1,8 m.

## 6.2 Parametric survey

A number of different parameters have been varied to see the impact they have on the load carrying capacity. Things that have not been tested are things connected to geometry of the arch, such as span, rise and arch barrel thickness. The reason for this is not that they do not play a role in the load carrying capacity as they of course do but that they are so to say “easy”, which is an overstatement, to measure. Neither have damages such as mortar loss and settlings been modelled. These can vary in an infinite number of ways and have to be implemented for each individual arch. Damages play a significant role in the load carrying capacity and leaving them out of this analysis should not be seen as an attempt to neglect them. More about how to model damages in RING2.0 and Archie-M can be found in chapter 7.

The parametric survey is made in both RING2.0 and Archie-M. The material parameters studied are changed, one by one. Except from material parameters the default settings for the programs are kept. This results in a difference in the live load dispersion method between the programs. RING2.0 uses the Boussinesq model while Archie-M uses a uniform method.

The Boussinesq dispersion model gives a “bell-shaped” load distribution which is a better approximation than a uniform distribution. LimitState (2009)

### 6.2.1 Method

In both programs the input of material and geometrical parameters are changed in similar ways. But there are differences for finding the worst load position.

#### 6.2.1.1 RING2.0

The geometry of the arch itself will be held constant with values according to Figures 6.5 and 6.6. A double axle bogie with the load 8 tonnes on each axle runs across the arch with steps of 1/99 of the span. For each step a load factor is calculated. The load factor is the multiplier on the load that leads to failure. One parameter at a time is changed and for each change the load factor is computed showing what affect the certain parameter has on the load carrying capacity. The failure mechanism is shown by the program, see Figure 6.7 and 6.8.

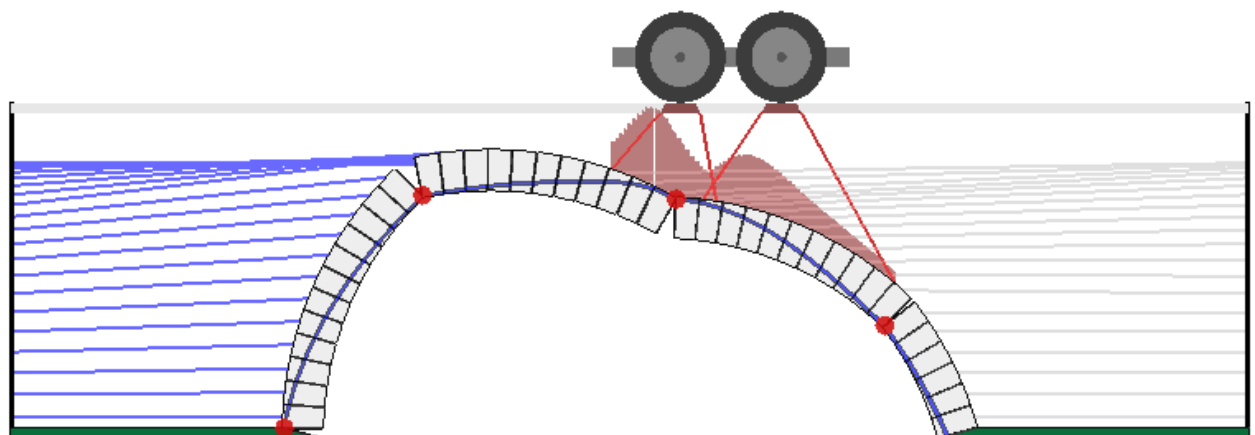


Figure 6.7 Failure mechanism for the Visman arch from RING2.0.

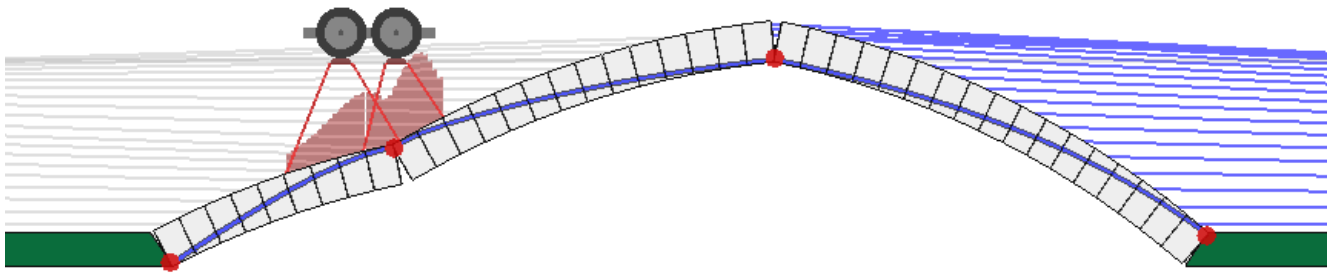


Figure 6.8 Failure mechanism for the Bridgemill arch from RING2.0.

### 6.2.1.2 Archie-M

The loading is the same and material properties are handled in the same manner in Archie-M as in RING2.0. The program calculates the worst position for the selected load automatically. The ultimate load carrying capacity is obtained by increasing the load factor until the zone of thrust touches the edge of the arch in a fourth point (in addition to the three pins that is symbolized as circles), see Figures 6.9 and 6.10 for the two bridges studied in this report. Sustainable bridges (2007)

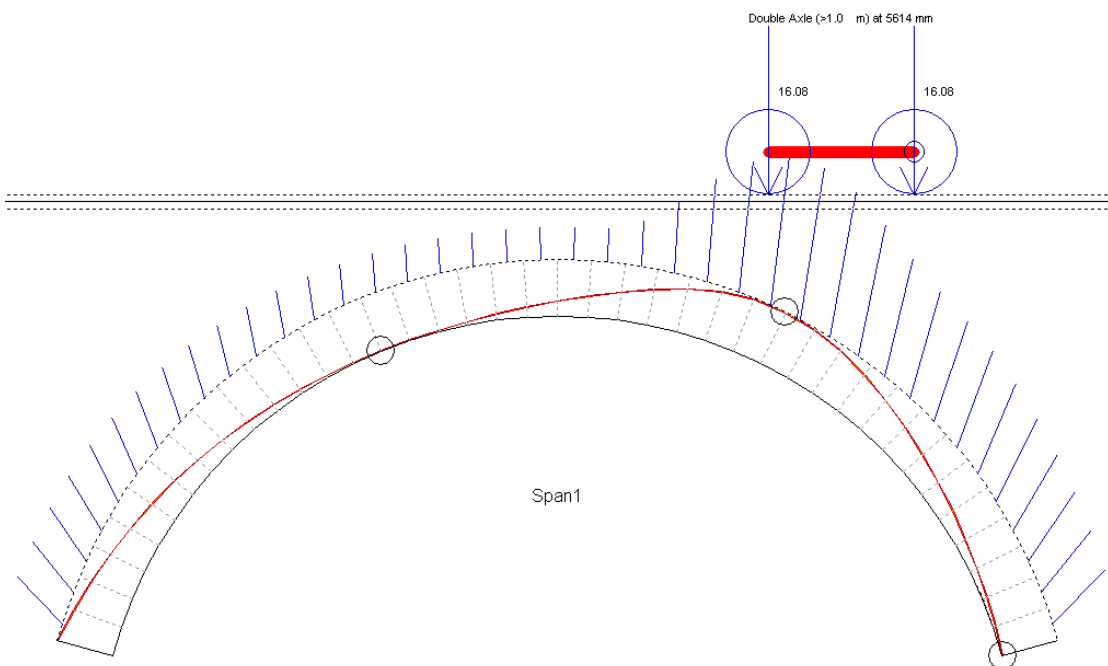


Figure 6.9 Limit state for the Visman arch, from Archie-M.

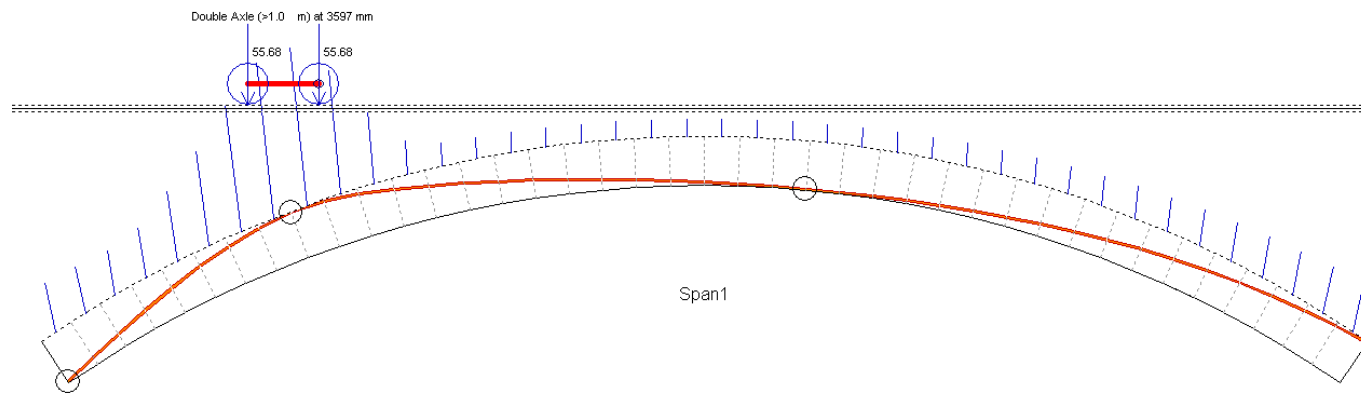


Figure 6.10 Limit state for the Bridgemill Bridge, from Archie-M.

Archie-M has some limitations that will make the comparison with RING2.0 incomplete. The limitations that will affect this comparison are that Archie-M does not have the possibility to model cohesion and the upper limit for compressive strength of masonry is 30 MPa in the program.

## 6.2.2 Results

The full parametric survey with ingoing parameters is shown in Appendix A. To make further comparisons of the results and other programs references will be made to two different parametric surveys, one made by Tóth A. R. et al. (2009), also mentioned in section 5 and another one made by Ng K-H. et al. (2004). Results obtained in this report can be compared to those to see what the correlation is between each parameter for the programs. It must be pointed out that there are significant differences in the geometry and set up of the bridges, so too long going conclusions of this comparison may be dangerous. But it is interesting to see if the behaviour of the parameter variation is similar.

The two parameters that Tóth A. R. et al. changed and that are possible to vary in RING2.0 and Archie-M is the friction angle and backfill cohesion. The material they started out with was sand with a unit weight of  $19 \text{ kN/m}^3$  which is quite close to the  $22 \text{ kN/m}^3$  that is the starting value here. Also the friction angle is close with a starting value of 37,5 degrees.

Results for the parametric survey from RING2.0 are seen in Table 6.4 and corresponding for Archie-M is shown in Table 6.5.

Table 6.4 Results from the parametric survey in Ring2.0 for the Visman arch.

Change the angle of friction

Masonry density	Compressive strength	Friction coefficient	Backfill density	Angle of friction	Cohesion	Fill height	Load factor
25	15	0,5	20	33	0	0,4	3,84
25	15	0,5	20	35	0	0,4	4,02
25	15	0,5	20	37	0	0,4	4,22
25	15	0,5	20	39	0	0,4	4,45
25	15	0,5	20	41	0	0,4	4,71
25	15	0,5	20	43	0	0,4	4,99
25	15	0,5	20	45	0	0,4	5,32

Table 6.5 Results from the parametric survey in Archie-M for the Visman arch.

Change the angle of friction

Masonry density	Compressive strength	Friction coefficient	Backfill density	Angle of friction	Fill height	Load factor
25	15	0,5	20	33	0,4	1,97
25	15	0,5	20	35	0,4	2,01
25	15	0,5	20	37	0,4	2,05
25	15	0,5	20	39	0,4	2,05
25	15	0,5	20	41	0,4	2,05
25	15	0,5	20	43	0,4	2,05
25	15	0,5	20	45	0,4	2,05

Results from both programs for both bridges have been drawn into a diagram, Figure 6.11.

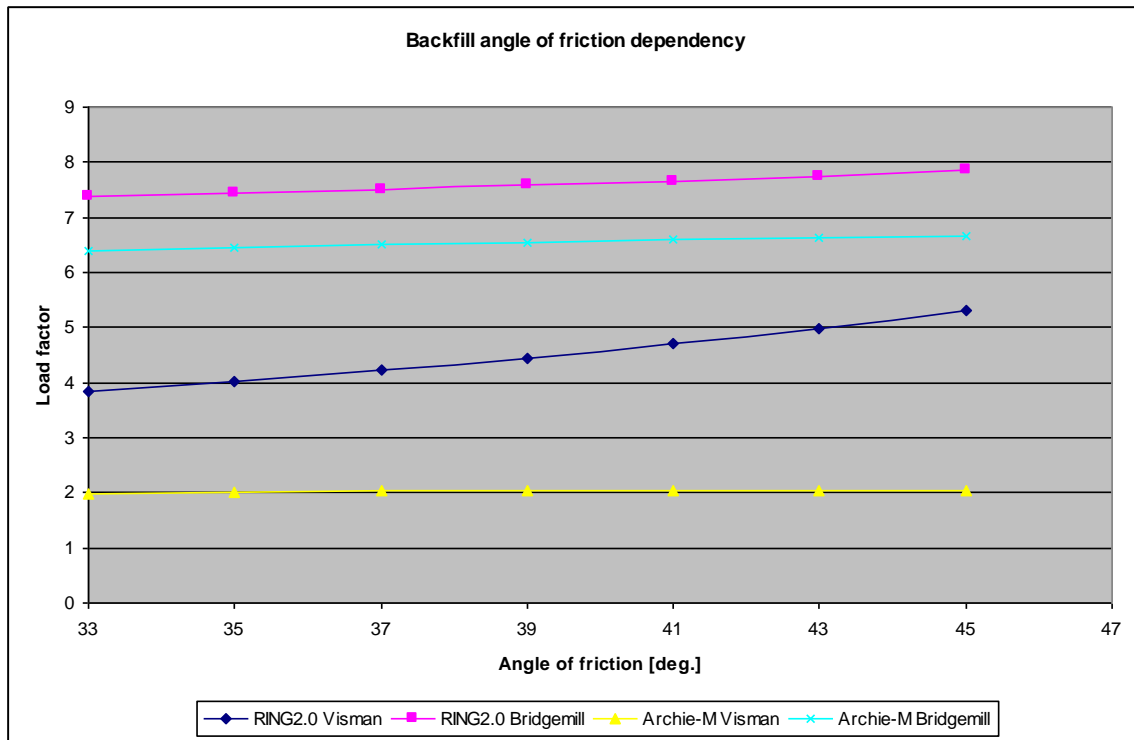


Figure 6.11 Load factor as a function of the angle of friction in RING2.0 and Archie-M

For the short span arch modelled in RING2.0 the increase in load carrying capacity is 38,5 percent and for the long span arch 6,5 percent. Corresponding numbers from Archie-M are 4,1 percent and 4,2 percent. Both the increase in load and the load factor are off regarding the Visman arch in Archie-M compared to RING2.0. For Bridgemill that have a longer span, the programs are in proximity to each other regarding both load factor and the increase in load factor caused by changing the angle of friction.

Tóth A. R. et al. (2009) have done the same survey using the software UDEC with the results in Figure 6.12.

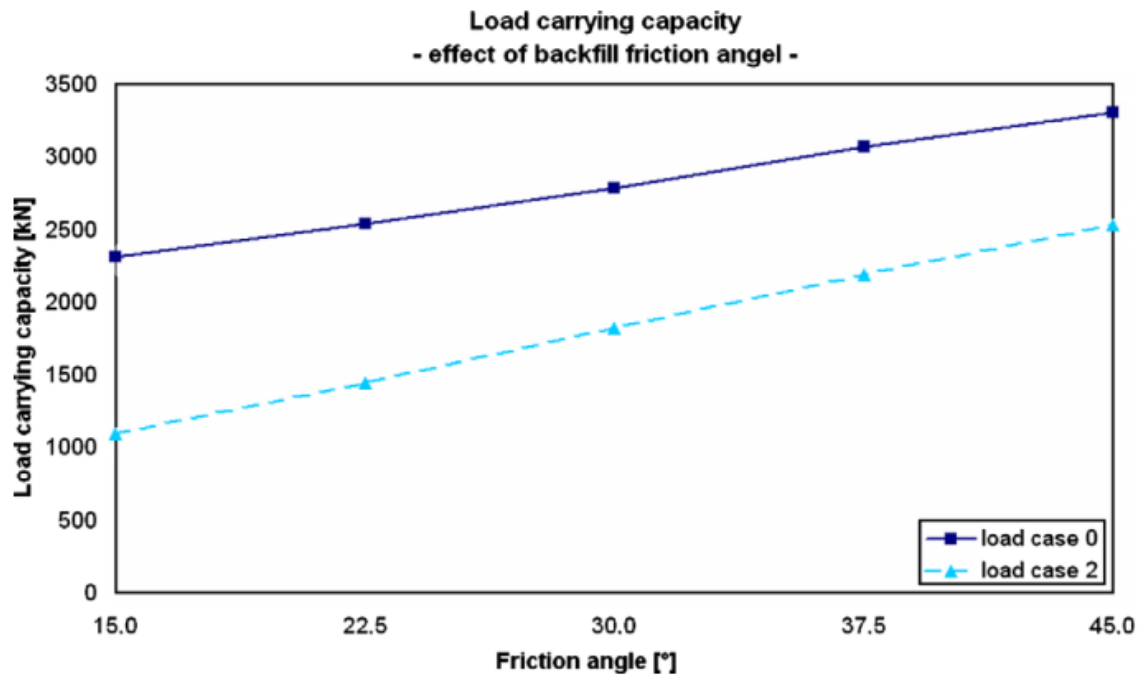


Figure 6.12 Load carrying capacity as a function of the angle of friction in UDEC. Tóth A. R. et al. (2009)

The behaviour of Tóth A. R. et al. (2009) results is quite similar to the one obtained in RING 2.0 for the Visman arch. The increase in the load carrying capacity, (only considering the interval 33-45 deg.) is around 25 percent for load case 0 and around 32 percent for load case 2. Load case 0 corresponds to a load in the middle of the span and load case 2 to a load in the quarter point. The span of the bridge studied by Tóth A. R. et al. (2009) is 11,36 m, which is closer to the Visman arch than Bridgemill. Load case 2 is a load applied close to the quarter point of the arch, in the same region where the Visman arch reaches the lowest load factor. So for the short span arch there is a good correlation between RING2.0 and UDEC.

Archie-M and RING2.0 have quite good correlation for the Bridgemill bridge, there is a difference between the load factors of about 15 percent were RING2.0 have the higher estimation of the load carrying capacity. The increase in load carrying capacity from changing the angle of friction is in the same region for the both programs for the Bridgemill bridge.

The other study that will be used for comparison with results from the parametric study is the study done by Ng K-H. et al. (2004). Their study used the previously mentioned Bargeower Bridge as study object and it was analysed with the mechanism method. Section 4 explained the basics of the mechanism method. Ng K-H. et al. (2004)

The modified mechanism method is only used to compare the obtained results from the present parametric study and is not presented more thoroughly.

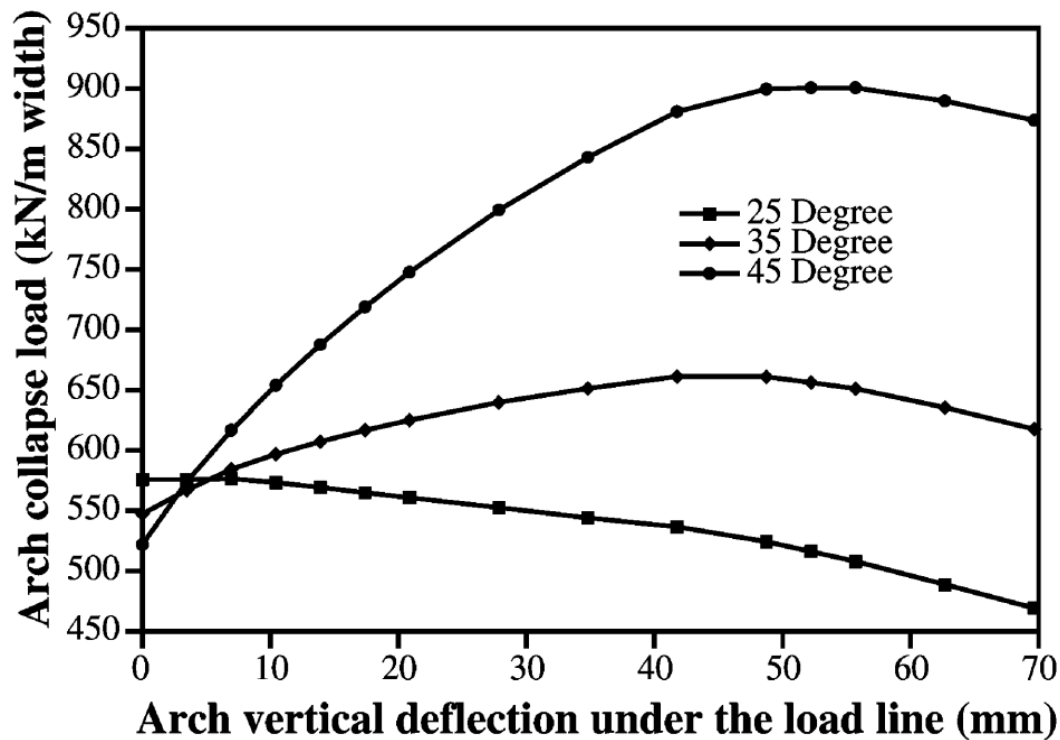


Figure 6.13 Load carrying capacity for different backfill angle of friction. Ng K-H. et al. (2004).

Figure 6.13 shows the results from the above mentioned study when altering the backfill materials angle of friction. When changing from 35 to 45 degrees the arch collapse load increased with 36 percent. Ng K-H. et al. (2004)

The second comparison that can be made is the dependence on the backfill cohesion properties. This parameter can't be specified in Archie-M so this comparison will only consider RING2.0. Figure 6.14 shows the effect on the load factor when the cohesion properties is changed in RING2.0. As shown, the cohesion does not influence the load factor in these simulations significantly. In appendix A the change is shown in numbers and it can be seen that the load factors increases a little.

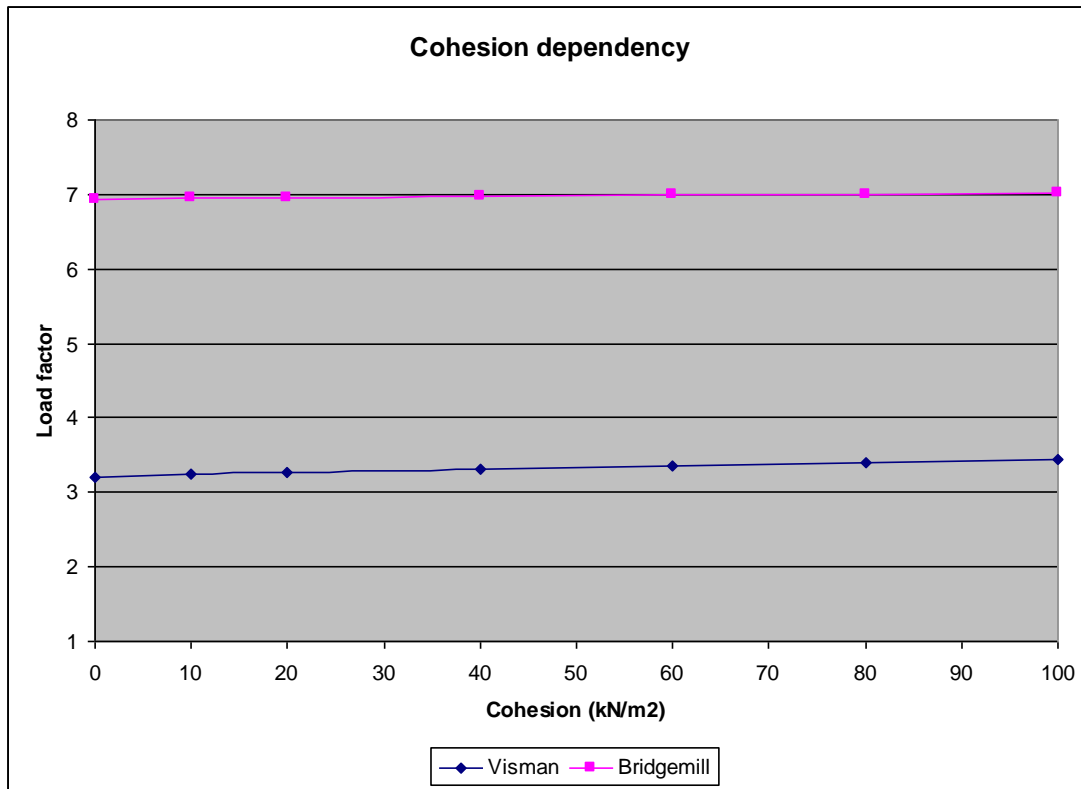


Figure 6.14 Load factor as a function of the backfill cohesion in RING2.0.

The behaviour found in RING2.0 is strange in light of the results from Tóth A. R. et al. That study show a great importance of the cohesion properties, Figure 6.15. It is also stated in their report that “Among the analyzed material characteristics the cohesion had the most significant effect on the load carrying capacity.

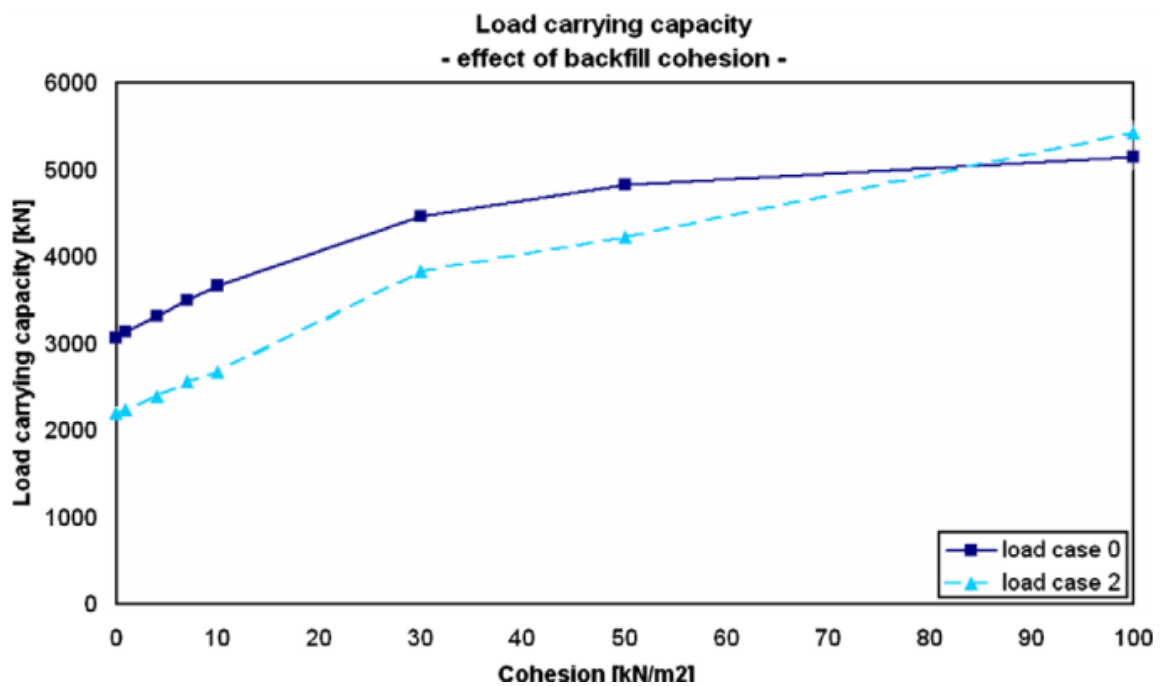


Figure 6.15 Load carrying capacity as a function of the cohesion, in UDEC. Tóth A. R. et al. (2009).

In chapter five, Figure 5.6 the correlation between UDEC and RING2.0 is shown. Clay 1 and Sand 1 have the same densities but differ in angle of friction and cohesion. Figure 6.16 show the results from different loadings on the same arch. It can be seen that for RING2.0 the curve for clay 1 lies just beneath the curve for sand 1 and they follow each other almost exactly for the different load cases. For the UDEC curves of the same materials the behaviour is very different, suggesting that RING2.0 not have the same sensitivity for cohesion as UDEC.

The reason for this is that the default value for the parameter  $m_{pc}$ , which is a multiplier on the effect of the cohesion, is 0.01, i.e. very conservative. This is done because the lack of information regarding the cohesion effect on the ultimate load of stone arch bridges. LimitState(2009).

Figure 6.16 presents results from the study made by Ng K-H. et al. (2004) and the influence from changed backfill unit weight.

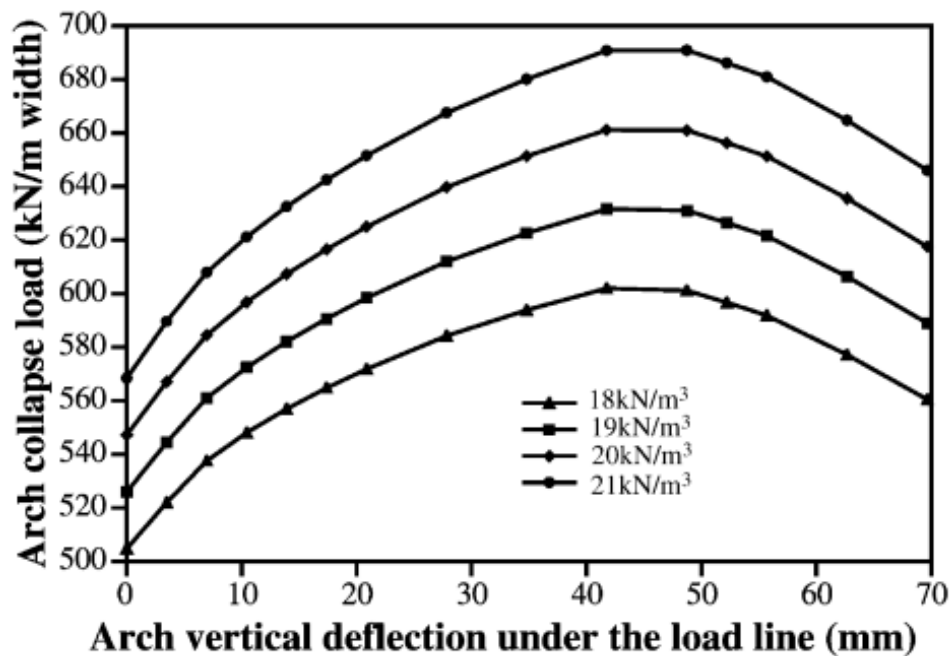


Figure 6.16 Collapse load – deflection relations for different backfill unit weight. Ng K-H. et al. (2004)

Their study showed an increase of the arch collapse load of about 15 percent when the backfill unit weight increased from 18 to 21 kN/m<sup>3</sup>.

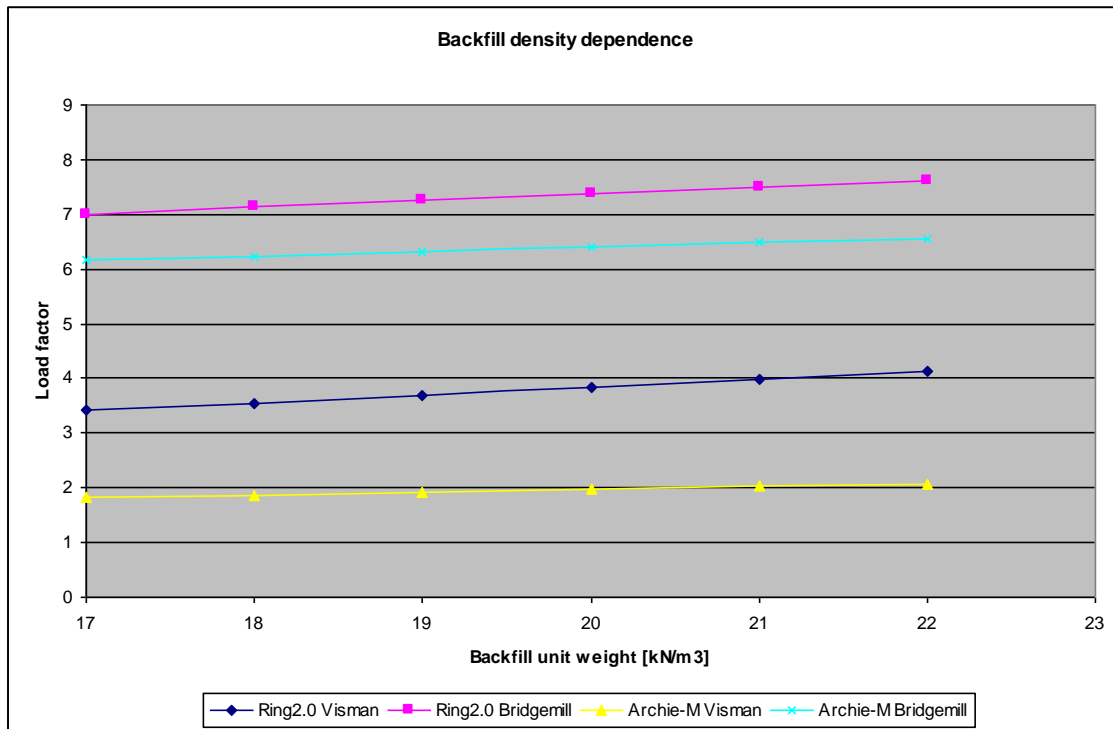


Figure 6.17 Load factor as a function of the backfill unit weight.

The parametric study in RING2.0 shows a 12 percent increase in the collapse load for the Visman arch and a 5 percent increase for the Bridgemill bridge. Corresponding values for Archie-M are 9 and 4 percent, Figure 6.17.

The result from the present model of the Visman arch in RING2.0 is the best corresponding with the results from the survey made of Ng. K-H. et al. (2004). The bridge they studied had a span of 10,4 m making it more similar to the Visman arch than the Bridgemill bridge.

Another investigated parameter is the arch material unit weight. This parameter has a small influence on the arch collapse load obtained by Ng. K-H. et al. (2004) , Figure 6.18. A unit weight increase from 19 to 22 kN/m<sup>3</sup> only raises the collapse load with 1.5 percent.

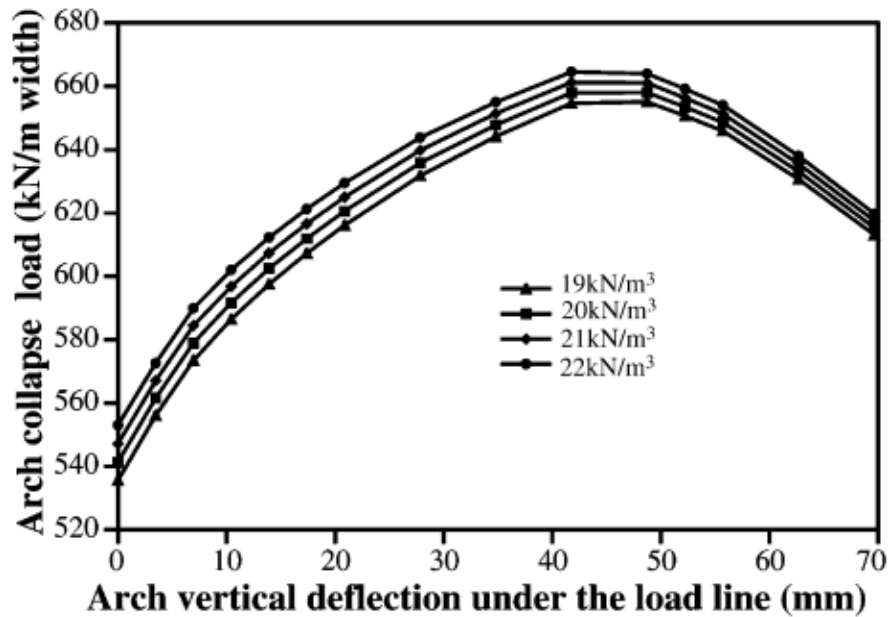


Figure 6.18 Collapse load – deflection relations for different arch material unit weight. Ng K-H. et al. (2004)

Similar values are obtained in RING2.0 and Archie-M. Closest is the RING2.0 model of the Visman arch with 1.8 percent increase of the ultimate load, and the three other give a higher increase of around 4 -5 percent, Figure 6.19.

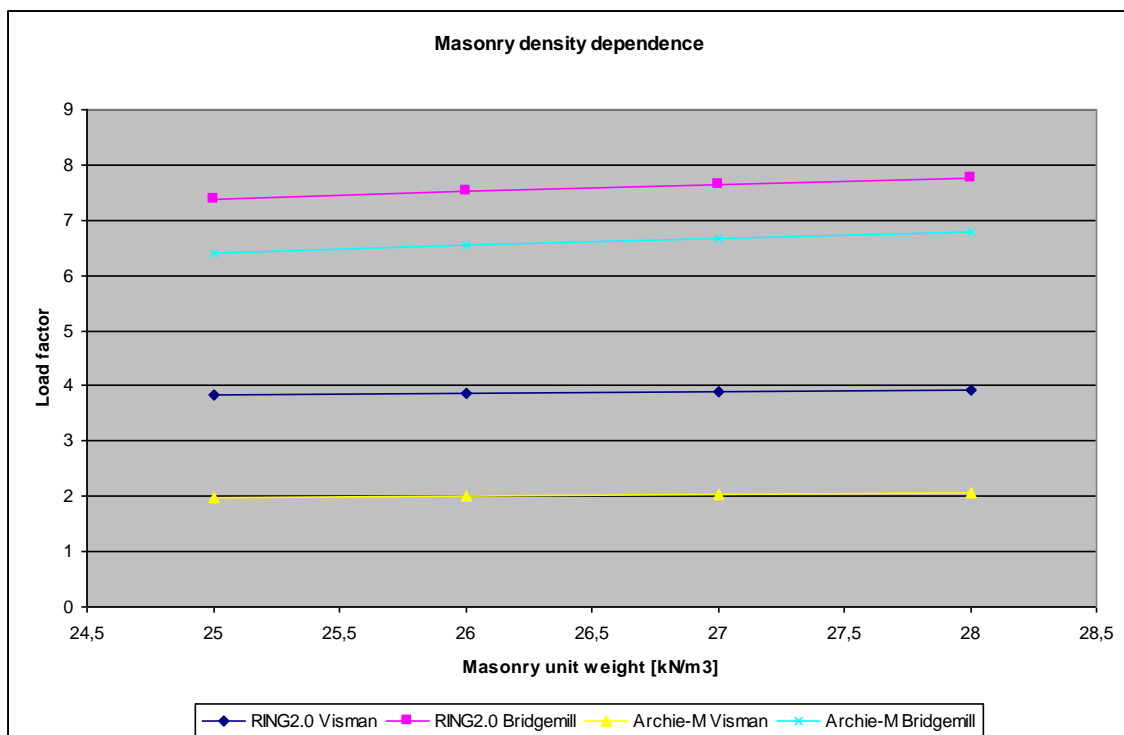


Figure 6.19 Load factor as a function of the masonry density.

Note that the interval of the masonry unit weight is not the same in the study made by Ng. K-H. et al. (2004) and the present study because of different materials in the

structure. However, the results are similar which implies that the masonry arch material unit weight is not a significant parameter.

Compressive strength dependency from the two different programs is shown in Figure 6.20.

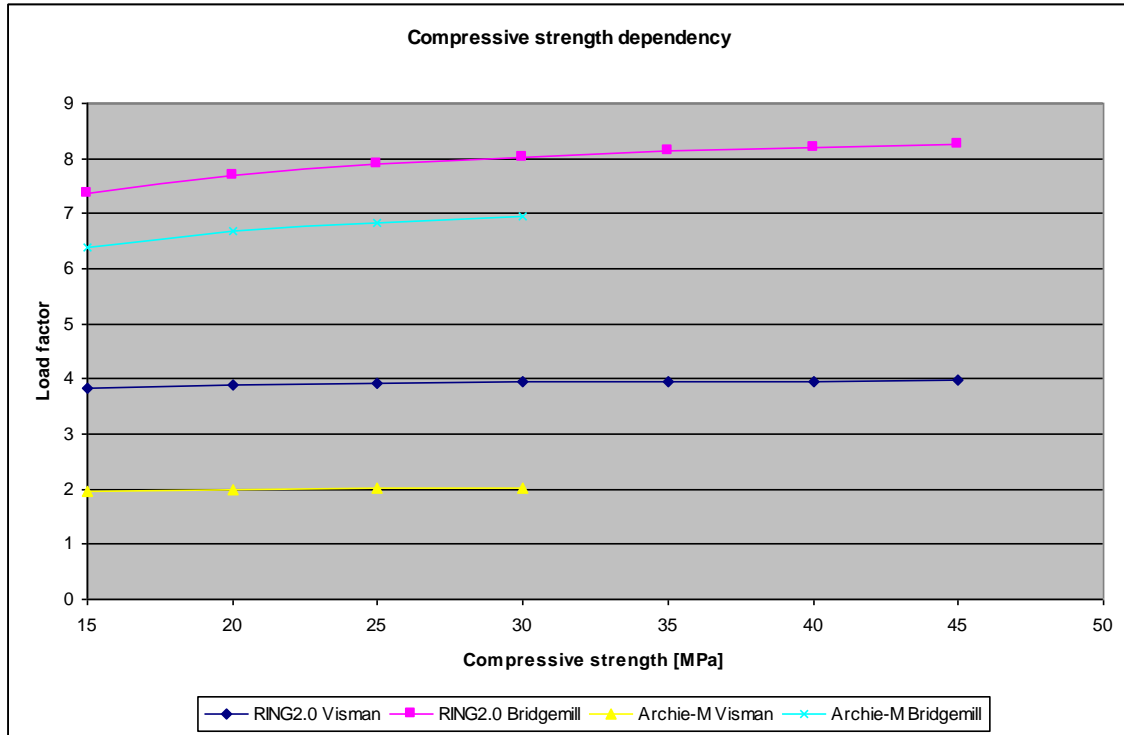


Figure 6.20 Load factor as a function of the compressive strength.

This parameter is not the most significant parameter, but it is the one parameter that gives the best correlation for the both programs. The increase in load carrying capacity for Visman arch is 2,6 percent in RING2.0 and 2,0 percent in Archie-M. Corresponding for Bridgemill is 8,8 and 8,9 percent. These results are only for compressive strengths up to 30 MPa were Archie-M has a limit on the compressive strength. On the other hand does a continued increase of the compressive strength give a low increment of the load carrying capacity.

The single most important parameter is the fill height of the backfill material, Figure 6.21.

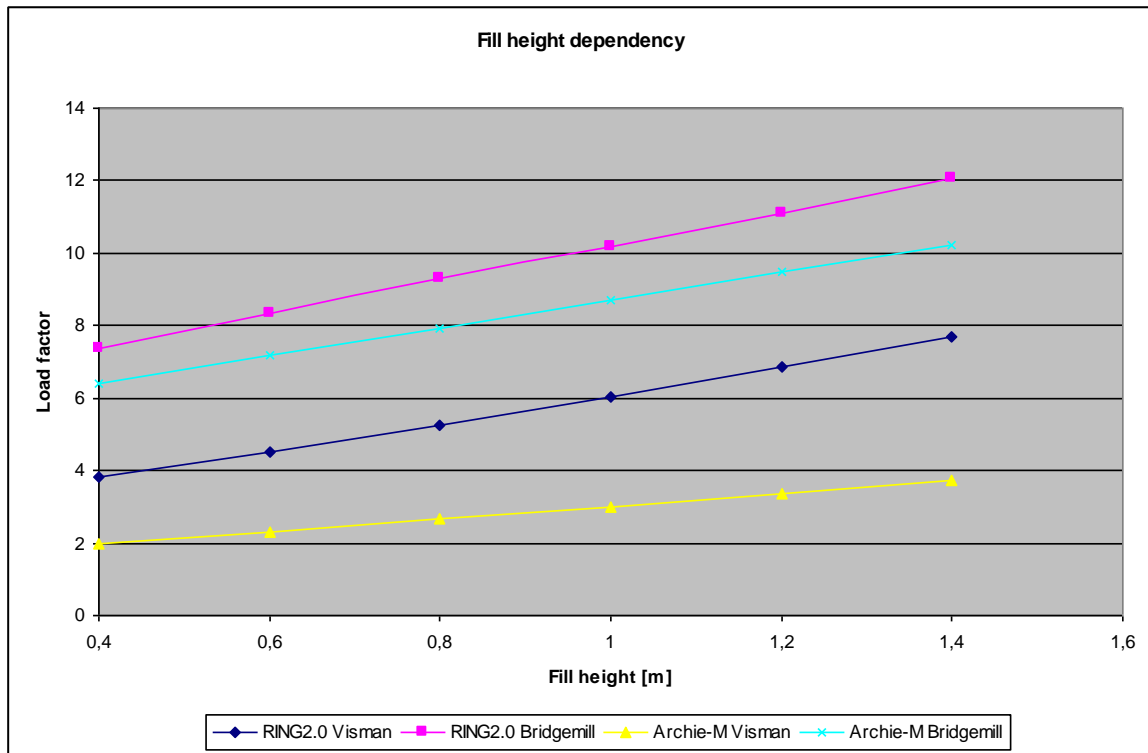


Figure 6.21 Load factor as a function of the fill height.

Also here is the increase in the load carrying capacity similar for the bridges in both programs. For the Visman arch the increase is 100 percent in RING2.0 and 90 percent in Archie-M and for Bridgemill respectively 63 and 60 percent.

### 6.2.3 Compilation of results

Table 6.4 show the results from the parametric study as the percentage increase when the material parameter is changed from it's lowest to it's highest within the intervals given.

Table 6.4 The result of the parametric study. Percentage of increase of the load carrying capacity when changing from the lowest to the highest value of the parameter.

	Archie-M		RING2.0	
	Bridgemill	Visman	Bridgemill	Visman
Angle of friction	4,2	4,1	6,5	38,5
Cohesion	-	-	1	7,5
Backfill unit weight	4	9	5	12
Arch barrel unit weight	6,1	4,6	5,3	1,8
Compressive strength	8,9	2	8,8	2,6
Fill height	60	90	63	100

## 7 Capacity calculation using design code standard vehicles

Design codes regulate the type of loading situations that is necessary to evaluate the bridge for. These vehicles are presented in a number of axle set-ups and can be found in Vägverket (1998) for the national roads. Similar models exist for railways. The simplest case is a single point load applied to the road surface and then the load cases becomes more complex. The load cases are denoted a) to l). Figure 7.1 and 7.2 show two different types of design code vehicles.

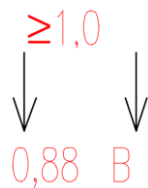


Figure 7.1 Design code vehicle b). Vägverket (1998)



Figure 7.2 Design code vehicle h). Vägverket (1998)

The factor  $B$  is the wanted parameter that describes the highest allowed bogie load. If any distributed load  $q$  is part of the vehicle this should either be set to 0 or 5 kN/m and evenly distributed over the lane. Loading  $B$  is equally distributed to the nearby axles and the centre width of the wheels should vary between 1,7 m and 2,3 m. The distributed length under the wheels should be 200 mm. Vägverket (1998)

The distributed loading can be applied in the programs by adding additional axles. There are questions about the appliance of the distributed loading part of the models on masonry arches. That is because of the origin of these models as derived from influence lines on beams. LimitState (2009)

Design code axle set up h), see Figure 7.2, will be used as an example of how these axle set up may be used in RING2.0. The input file to get the loading situation into RING2.0 is appended in Appendix B. The bogie reference load  $B$  is set to 1 kN and the distributed loads are set to zero.

The resulting critical load case is shown in Figure 7.3. The load factor for this critical case is 1072.8, this means that the critical load is 1072.8 kN (110 tonnes) because the assumption that the reference load B is equal to 1 kN in the input file.

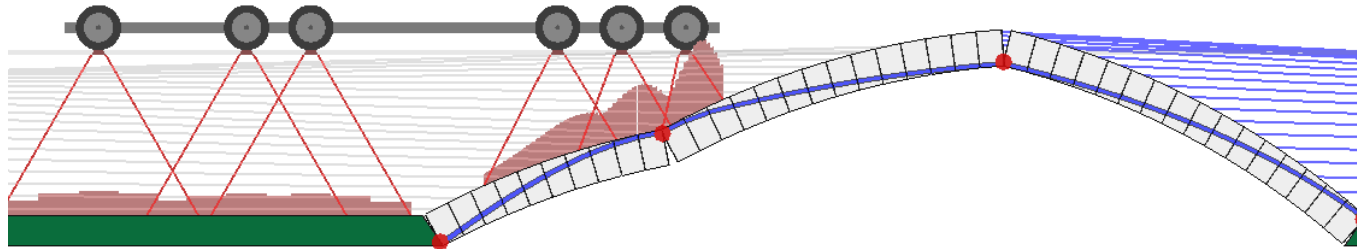


Figure 7.3 Critical load case for the design code axle set up h) on the Bridgemill bridge calculated in RING2.0.

The same calculation for design code axle set up h), also here without the distributed loading, has been done in Archie-M. The input file and explanation of it can be seen in appendix C. Figure 7.4 show the result from the worst case loading position.

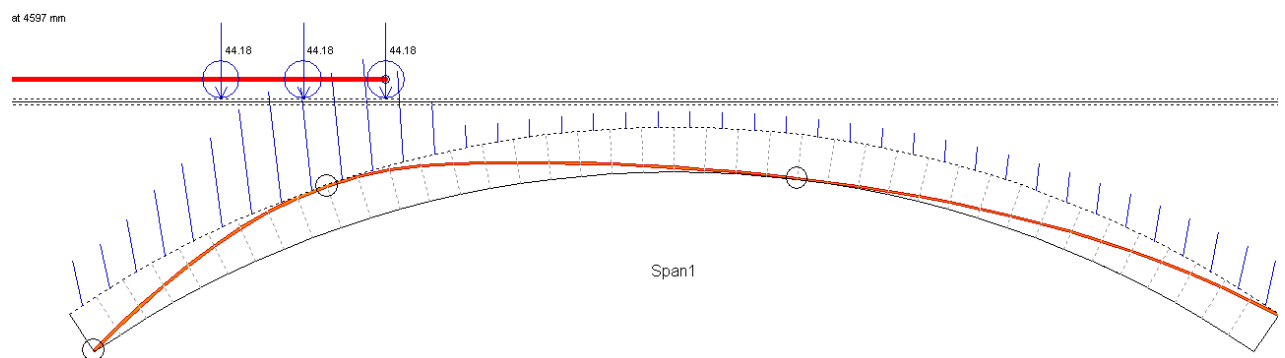
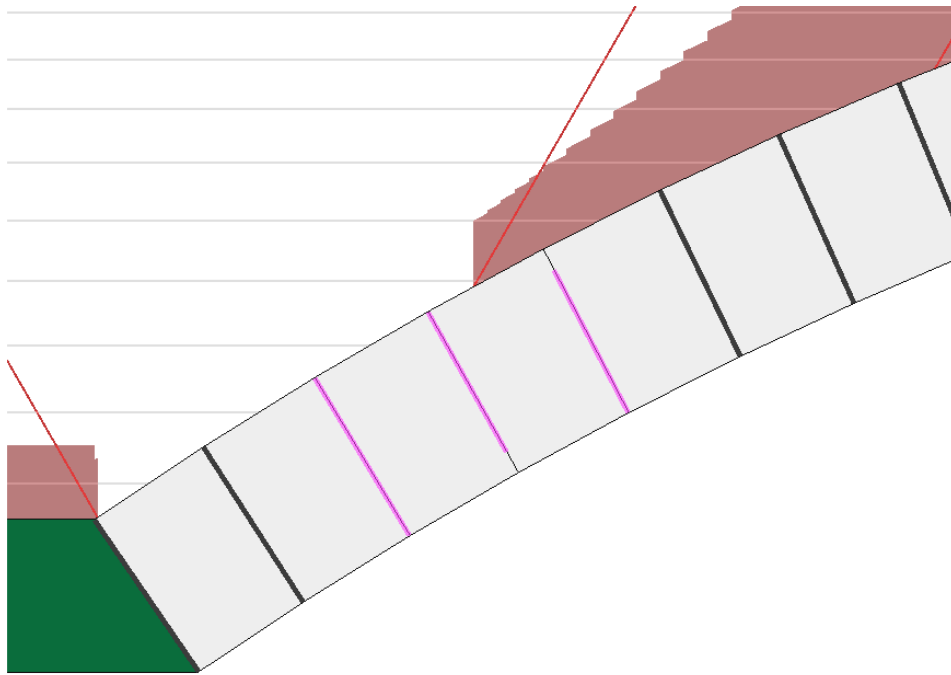


Figure 7.4 Critical load case for the design code axle set up h) on the Bridgemill bridge calculated in Archie-M.

The resulting load factor in Archie-M is 985, which means that the critical load is 985 kN (100 tonnes), just a ten percent difference from the value obtained in RING2.0.

## 7.1 Damages

The above calculated allowed bogie load is for the perfect case and with no safety factors applied. A real bridge will probably have deteriorations and flaws to the structure. RING2.0 has the possibility to model loss of mortar in the joints. In Figure 7.5 the arch have three joints highlighted, the first one is a joint with no mortar loss, the second one have a 90 mm mortar loss from the intrados and the last one have a 90 mm mortar loss from the extrados.



*Figure 7.5 Mortar loss modelled in RING2.0.*

This feature also gives the possibility to change the crushing strength and friction coefficient for selected joints. The reduction of mortar material can also be used to take cracks into account because the reduction of arch barrel height. LimitState (2009).

Archie-M also give the possibility to model mortar loss but this can only be done with the same value over the whole arch and not on a individual basis as in RING2.0. No local defects can be modelled in Archie-M. Sustainable bridges (2007).

Both programs give the option to model the true shape of the arch in order to take settlements and distortions to the geometry into account in the analysis.

## 8 Conclusions

Other reports referred to in this thesis have shown that it is possible to model masonry arch bridges and obtain reasonable results compared to reality. What this study has done is to investigate what methods that are available for masonry arch calculations. Material parameters with great influence on the load carrying capacity have also been identified.

### 8.1 Preferable method of load carrying calculation

There are as shown a number of different ways to perform a load carrying calculation. In this thesis have the two commercial programs, Archie-M and RING2.0, been used for calculations. Both these programs are very user – friendly and can be quickly learned. Easy input and fast running analysis grant that many analyses's can be done for e.g. making it possible to make parametric studies to see what influence different parameters will have on the load carrying capacity. The parametric study done in this thesis show that the two programs give different results for the same case. It is impossible to say which one, if any, of the programs that is right. To get some kind of verification it can be wise to use some other method like three dimensional FEM and compare the results.

What can be said is that LimitState (2009) presents a range of examples of real bridges and laboratory testing that shows a good correspondence with computational results. RING2.0 comes with a "Theory and modelling guide" LimitState (2009) that contains valuable information about many issues that an engineer can come across during masonry arch calculations. The output from RING2.0 in form of the load factor is easy to interpret. All these things make RING2.0 a very interesting choice as the preferred program of load carrying calculation.

### 8.2 Crucial parameters of assessment

The single most important parameter tested is the fill height. A one meter increase in fill height gave between 60 and 100 percent higher load carrying capacity. This parameter can also be claimed to be part of the geometry and "easy" to measure. It is something that is possible to change on a bridge in reality in contrast to the arch barrel thickness etc.

Among the material parameters there is no one that gives dramatic changes to the load carrying capacity in the simulations. The only thing that gives a dramatic change is when the angle of friction is raised to 45 degrees for the Visman arch in RING2.0. Once again it is hard to say whether it is right or not, but Archie-M give a much lower result. On the other hand have the simulation in UDEC by Tóth A et al. (2009). given almost the same result. Also the modified mechanism method made by Ng K-H. et al. (2004) gave an increase of arch collapse load in the vicinity to the result from RING2.0. What these three results have in common are that they come from bridges with a span/rise ratio of around 2 (Visman=2.6, Tóth A.R. et al~2.2, Bargeower= 2). For a bridge of that kind with a high rise the arch have more backfill to "work against" which is the reason why this type of bridge show a high increase in the load carrying capacity when the backfills angle of friction is increased. In light of the three different simulations showing a high dependence on the backfill angle of friction for

high rise bridges, the result from Archie-M seem strange. The same variation there gave only an increase in load carrying capacity of 4.1 percent.

The angle of friction is the only parameter for which the difference between the programs is significant.

To make an accurate model it is of course of great importance to have as good information as possible. If all material parameters are off, the result will be off too. A five to ten percent change for each parameter which is the result from the parametric study could give greater impact when combined. Therefore it is suggested that the properties of the backfill is investigated as thoroughly as necessary for the actual case compared with effort and budget.

For the arch barrel it is only the compressive strength that can vary vastly according to the information showed in this report. Density is similar for all granite, but with larger joints the density of the composite will be lower.

One important thing that must be stressed is that it is important to take damages in the construction into account.

It is, as the comparison with full scale tests showed, possible to achieve good predictions of the load carrying capacity.

## 9 References

- Institution of Civil Engineers ICE (2008): *ICE Manual of Bridge Engineering*, Thomas Telford, London, 748 pp
- Samuelsson A. Wiberg N-E. (1995): *Byggnadsmekanik - Strukturmekanik* (Building mechanic – structural mechanic. In Swedish), Chalmers, Göteborg,
- Choo B. S. Coutie M. G. Gong N. G. (1991): *Finite element analysis of masonry arch bridges using tapered elements. Proc. Instn. Civ. Engrs. Part 2*, 91 pp.
- LimitState (2009): *RING Theory and modelling guide*. LimitState, Sheffield, 88 pp.
- Heyman (1982): *The masonry arch Ellis Horwood series in engineering science*, Ellis Horwood, Chichester, 117 pp
- Sustainable bridges (2004): *European railway bridge demography D1.2*. European commission. 15 pp.
- Sustainable bridges (2007): *Methods of analysis of damaged masonry arch bridges Background document D4.7.3*, European commission, 71 pp.
- Banverket (2005): *Bärighetsberäkning av järnvägsbroar BVS 583.11*, (Load carrying calculation of railway bridges BVS 583.11. In Swedish), Banverket, Borlänge, 136 pp.
- Vägverket (1998): *Allmän teknisk beskrivning för klassningsberäkning av vägbroar Publ. 1998:78*, (General technical descriptions for assessment calculations of road bridges Publ. 1998:78. In Swedish), Vägverket, Borlänge, 113 pp.
- Vägverket (2010[1]): *Tekniska kravdokument geo. Publ. 2009:46*. (Technical requirement documents. Publ 2009:46. In Swedish) Vägverket, Borlänge, 156 pp.
- Vägverket (2005): *Nationell plan för bevaransvärda broar. Publ. 2005:151*. (National plan for culturally valuable bridges. Publ. 2005:151, In Swedish) Vägverket, Borlänge, 142 pp
- The Highways Agency (2001): *Design manual for roads and bridges Volume 3 Highway structures: Inspection and maintenance Section 4 Assessment BA 16/97 Amendment no.2*. The highways agency, Richmond, 83 pp
- Toth A. Orbán Z. Bagi K. (2009): *Discrete element analysis of a stone masonry arch*. Mechanics Research Communications. 9 pp.
- Giordano A. Mele E. De Luca A. (2002): Modelling of historical masonry structures: comparison of different approaches through a case study. *Engineering Structures*, Volume 24, Issue 8, August 2002, Pages 1057-106

- Schlegel R. Rautenstrauch K. (2004): Comparative computations of masonry arch bridges using continuum and discontinuum mechanics. *Numerical Modelling of Discrete Materials in Geotechnical Engineering, Civil Engineering and Earth Sciences. Proceedings of the First International UDEC/3DEC Symposium, Bochum*. 4 pp.
- Lemos J.V.. (2004): Modeling stone masonry dynamics with 3DEC. *Numerical Modelling of Discrete Materials in Geotechnical Engineering, Civil Engineering and Earth Sciences. Proceedings of the First International UDEC/3DEC Symposium, Bochum*. 7 pp.
- Vasconcelos G. Lourenco P. B. (2009): Experimental characterization of stone masonry in shear and compression. *Construction and building materials*. Volume 23. Pages 3337 – 3345.
- Ng K-H. Fairfield C. A. (2004): Modifying the mechanism method of masonry arch bridge analysis. *Construction and Building Materials*, Volume 18, Issue 2, March 2004, Pages 91-97
- Crisfield M. A. Packham A. J. (1987): *A mechanism program for computing the strength of masonry arch bridges. TRRL research report 124*. TRRL. Crowthorne. 20 pp.
- Berndtsson E. Berndtsson J. Sandberg J. (1999): *3D- analys av stenbågbro med explicit FE-program*. (3D- analysis of stone arch bridge using explicit FE-program. In Swedish), Chalmers, Göteborg, 92 pp.
- Nationalencyklopedin (2010[1]): Pont du Gard (In Swedish). <http://www.ne.se> (2010-03-25)
- Nationalencyklopedin (2010[2]): Ponte Vecchio (In Swedish). <http://www.ne.se> (2010-03-25)
- Nationalencyklopedin (2010[3]): Kvader (In Swedish). <http://www.ne.se> (2010-03-26)
- Encyclopaedia Britannica (2010): bulk density: basalt, granite, sandstone. <http://www.britannica.com/EBchecked/topic-art/505970/2451/Dry-density-distribution-of-three-different-rock-types-basalt-granite> (2010-03-29)
- Wikipedia (2010): *Zhaozhou bridge* [http://en.wikipedia.org/wiki/Zhaozhou\\_Bridge](http://en.wikipedia.org/wiki/Zhaozhou_Bridge) (2010-05-05)
- Swedgeo (2010): *Jordarter* (Soil types. In Swedish) [http://www.swedgeo.se/templates/SGIStandardPage\\_\\_\\_\\_1098.aspx?epslanguage=SV](http://www.swedgeo.se/templates/SGIStandardPage____1098.aspx?epslanguage=SV) (2010-03-29)
- Connecticut's historic highway bridges (2010) Stone arch bridges. <http://www.past-inc.org/historic-bridges/Mainpage.html> (2010-04-22)
- Vägverket (2010[2]): Extract from BaTMan (Bridge and Tunnel Management). Konstruktionstyp/material (construction type/ material) in Swedish.



## Appendix A

### Parametric study of the loadcarrying capacity, RING2.0

#### Visman arch

Change the density of the backfill

Masonry density	Compressive strength	Friction coefficient	Backfill density	Angle of friction	Cohesion	Fill height	Load factor
25	15	0,5	17	33	0	0,4	3,41
25	15	0,5	18	33	0	0,4	3,55
25	15	0,5	19	33	0	0,4	3,7
25	15	0,5	20	33	0	0,4	3,84
25	15	0,5	21	33	0	0,4	3,98
25	15	0,5	22	33	0	0,4	4,12

Change the density of the masonry

Masonry density	Compressive strength	Friction coefficient	Backfill density	Angle of friction	Cohesion	Fill height	Load factor
25	15	0,5	20	33	0	0,4	3,84
26	15	0,5	20	33	0	0,4	3,86
27	15	0,5	20	33	0	0,4	3,89
28	15	0,5	20	33	0	0,4	3,91

Change the angle of friction

Masonry density	Compressive strength	Friction coefficient	Backfill density	Angle of friction	Cohesion	Fill height	Load factor
25	15	0,5	20	33	0	0,4	3,84
25	15	0,5	20	35	0	0,4	4,02
25	15	0,5	20	37	0	0,4	4,22
25	15	0,5	20	39	0	0,4	4,45
25	15	0,5	20	41	0	0,4	4,71
25	15	0,5	20	43	0	0,4	4,99
25	15	0,5	20	45	0	0,4	5,32

Change the cohesion

Masonry density	Compressive strength	Friction coefficient	Backfill density	Angle of friction	Cohesion	Fill height	Load factor
25	15	0,5	17	30	0	0,4	3,21
25	15	0,5	17	30	10	0,4	3,24
25	15	0,5	17	30	20	0,4	3,26
25	15	0,5	17	30	40	0,4	3,31
25	15	0,5	17	30	60	0,4	3,36
25	15	0,5	17	30	80	0,4	3,4
25	15	0,5	17	30	100	0,4	3,45

### Change the compressive strength

Masonry density	Compressive strength	Friction coefficient	Backfill density	Angle of friction	Cohesion	Fill height	Load factor
25	15	0,5	20	33	0	0,4	3,84
25	20	0,5	20	33	0	0,4	3,89
25	25	0,5	20	33	0	0,4	3,91
25	30	0,5	20	33	0	0,4	3,94
25	35	0,5	20	33	0	0,4	3,95
25	40	0,5	20	33	0	0,4	3,96
25	45	0,5	20	33	0	0,4	3,97

### Change the fill height

Masonry density	Compressive strength	Friction coefficient	Backfill density	Angle of friction	Cohesion	Fill height	Load factor
25	15	0,5	20	33	0	0,4	3,84
25	15	0,5	20	33	0	0,6	4,52
25	15	0,5	20	33	0	0,8	5,27
25	15	0,5	20	33	0	1	6,05
25	15	0,5	20	33	0	1,2	6,87
25	15	0,5	20	33	0	1,4	7,68

## Bridgemill

### Change the density of the backfill

Masonry density	Compressive strength	Friction coefficient	Backfill density	Angle of friction	Cohesion	Fill height	Load factor
25	15	0,5	17	33	0	0,4	7
25	15	0,5	18	33	0	0,4	7,13
25	15	0,5	19	33	0	0,4	7,25
25	15	0,5	20	33	0	0,4	7,38
25	15	0,5	21	33	0	0,4	7,5
25	15	0,5	22	33	0	0,4	7,62

### Change the density of the masonry

Masonry density	Compressive strength	Friction coefficient	Backfill density	Angle of friction	Cohesion	Fill height	Load factor
25	15	0,5	20	33	0	0,4	7,38
26	15	0,5	20	33	0	0,4	7,51
27	15	0,5	20	33	0	0,4	7,64
28	15	0,5	20	33	0	0,4	7,77

### Change the angle of friction

Masonry density	Compressive strength	Friction coefficient	Backfill density	Angle of friction	Cohesion	Fill height	Load factor
25	15	0,5	20	33	0	0,4	7,38
25	15	0,5	20	35	0	0,4	7,44
25	15	0,5	20	37	0	0,4	7,5
25	15	0,5	20	39	0	0,4	7,58
25	15	0,5	20	41	0	0,4	7,66
25	15	0,5	20	43	0	0,4	7,75
25	15	0,5	20	45	0	0,4	7,86

### Change the cohesion

Masonry density	Compressive strength	Friction coefficient	Backfill density	Angle of friction	Cohesion	Fill height	Load factor
25	15	0,5	17	30	0	0,4	6,94
25	15	0,5	17	30	10	0,4	6,95
25	15	0,5	17	30	20	0,4	6,96
25	15	0,5	17	30	40	0,4	6,97
25	15	0,5	17	30	60	0,4	6,99
25	15	0,5	17	30	80	0,4	7
25	15	0,5	17	30	100	0,4	7,01

### Change the compressive strength

Masonry density	Compressive strength	Friction coefficient	Backfill density	Angle of friction	Cohesion	Fill height	Load factor
25	15	0,5	20	33	0	0,4	7,38
25	20	0,5	20	33	0	0,4	7,7
25	25	0,5	20	33	0	0,4	7,9
25	30	0,5	20	33	0	0,4	8,03
25	35	0,5	20	33	0	0,4	8,13
25	40	0,5	20	33	0	0,4	8,21
25	45	0,5	20	33	0	0,4	8,27

### Change the fill height

Masonry density	Compressive strength	Friction coefficient	Backfill density	Angle of friction	Cohesion	Fill height	Load factor
25	15	0,5	20	33	0	0,4	7,38
25	15	0,5	20	33	0	0,6	8,32
25	15	0,5	20	33	0	0,8	9,28
25	15	0,5	20	33	0	1	10,2
25	15	0,5	20	33	0	1,2	11,12
25	15	0,5	20	33	0	1,4	12,05

# Parametric study of the loadcarrying capacity, Archie-M

## Visman arch

Change the density of the backfill

Masonry density	Compressive strength	Friction coefficient	Backfill density	Angle of friction	Fill height	Load factor
25	15	0,5	17	33	0,4	1,82
25	15	0,5	18	33	0,4	1,87
25	15	0,5	19	33	0,4	1,92
25	15	0,5	20	33	0,4	1,97
25	15	0,5	21	33	0,4	2,03
25	15	0,5	22	33	0,4	2,08

Change the density of the masonry

Masonry density	Compressive strength	Friction coefficient	Backfill density	Angle of friction	Fill height	Load factor
25	15	0,5	20	33	0,4	1,97
26	15	0,5	20	33	0,4	2
27	15	0,5	20	33	0,4	2,03
28	15	0,5	20	33	0,4	2,06

Change the angle of friction

Masonry density	Compressive strength	Friction coefficient	Backfill density	Angle of friction	Fill height	Load factor
25	15	0,5	20	33	0,4	1,97
25	15	0,5	20	35	0,4	2,01
25	15	0,5	20	37	0,4	2,05
25	15	0,5	20	39	0,4	2,05
25	15	0,5	20	41	0,4	2,05
25	15	0,5	20	43	0,4	2,05
25	15	0,5	20	45	0,4	2,05

Change the compressive strength

Masonry density	Compressive strength	Friction coefficient	Backfill density	Angle of friction	Fill height	Load factor
25	15	0,5	20	33	0,4	1,97
25	20	0,5	20	33	0,4	1,99
25	25	0,5	20	33	0,4	2,01
25	30	0,5	20	33	0,4	2,01
25	35	0,5	20	33	0,4	
25	40	0,5	20	33	0,4	
25	45	0,5	20	33	0,4	

### Change the fill height

Masonry density	Compressive strength	Friction coefficient	Backfill density	Angle of friction	Fill height	Load factor
25	15	0,5	20	33	0,4	1,97
25	15	0,5	20	33	0,6	2,32
25	15	0,5	20	33	0,8	2,67
25	15	0,5	20	33	1	3
25	15	0,5	20	33	1,2	3,36
25	15	0,5	20	33	1,4	3,74

## Bridgemill

### Change the density of the backfill

Masonry density	Compressive strength	Friction coefficient	Backfill density	Angle of friction	Fill height	Load factor
25	15	0,5	17	33	0,4	6,16
25	15	0,5	18	33	0,4	6,23
25	15	0,5	19	33	0,4	6,31
25	15	0,5	20	33	0,4	6,39
25	15	0,5	21	33	0,4	6,48
25	15	0,5	22	33	0,4	6,56

### Change the density of the masonry

Masonry density	Compressive strength	Friction coefficient	Backfill density	Angle of friction	Fill height	Load factor
25	15	0,5	20	33	0,4	6,39
26	15	0,5	20	33	0,4	6,56
27	15	0,5	20	33	0,4	6,67
28	15	0,5	20	33	0,4	6,78

### Change the angle of friction

Masonry density	Compressive strength	Friction coefficient	Backfill density	Angle of friction	Fill height	Load factor
25	15	0,5	20	33	0,4	6,39
25	15	0,5	20	35	0,4	6,45
25	15	0,5	20	37	0,4	6,5
25	15	0,5	20	39	0,4	6,55
25	15	0,5	20	41	0,4	6,6
25	15	0,5	20	43	0,4	6,63
25	15	0,5	20	45	0,4	6,66

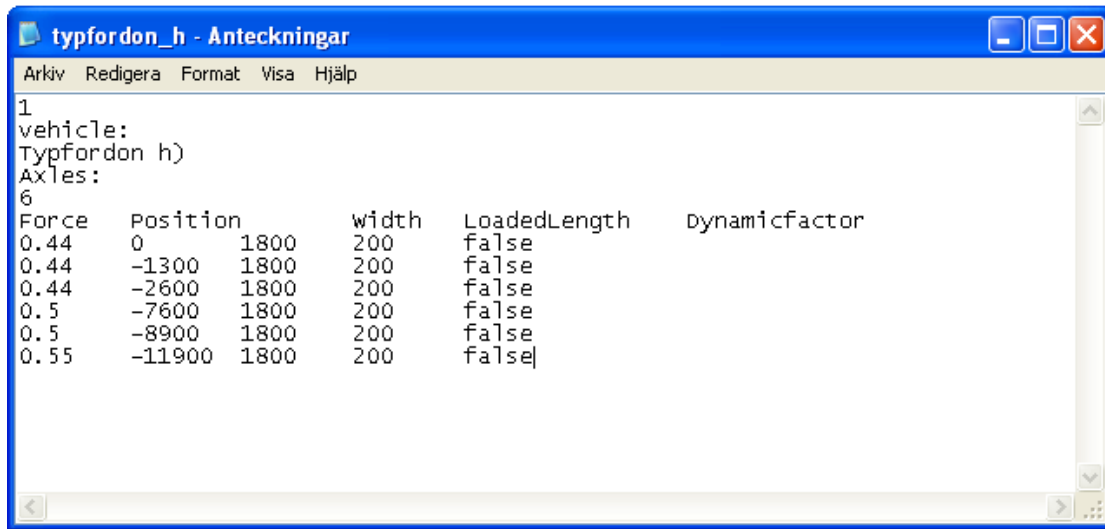
### Change the compressive strength

Masonry density	Compressive strength	Friction coefficient	Backfill density	Angle of friction	Fill height	Load factor
25	15	0,5	20	33	0,4	6,39
25	20	0,5	20	33	0,4	6,67
25	25	0,5	20	33	0,4	6,84
25	30	0,5	20	33	0,4	6,96
25	35	0,5	20	33	0,4	
25	40	0,5	20	33	0,4	
25	45	0,5	20	33	0,4	

### Change the fill height

Masonry density	Compressive strength	Friction coefficient	Backfill density	Angle of friction	Fill height	Load factor
25	15	0,5	20	33	0,4	6,39
25	15	0,5	20	33	0,6	7,18
25	15	0,5	20	33	0,8	7,94
25	15	0,5	20	33	1	8,69
25	15	0,5	20	33	1,2	9,48
25	15	0,5	20	33	1,4	10,21

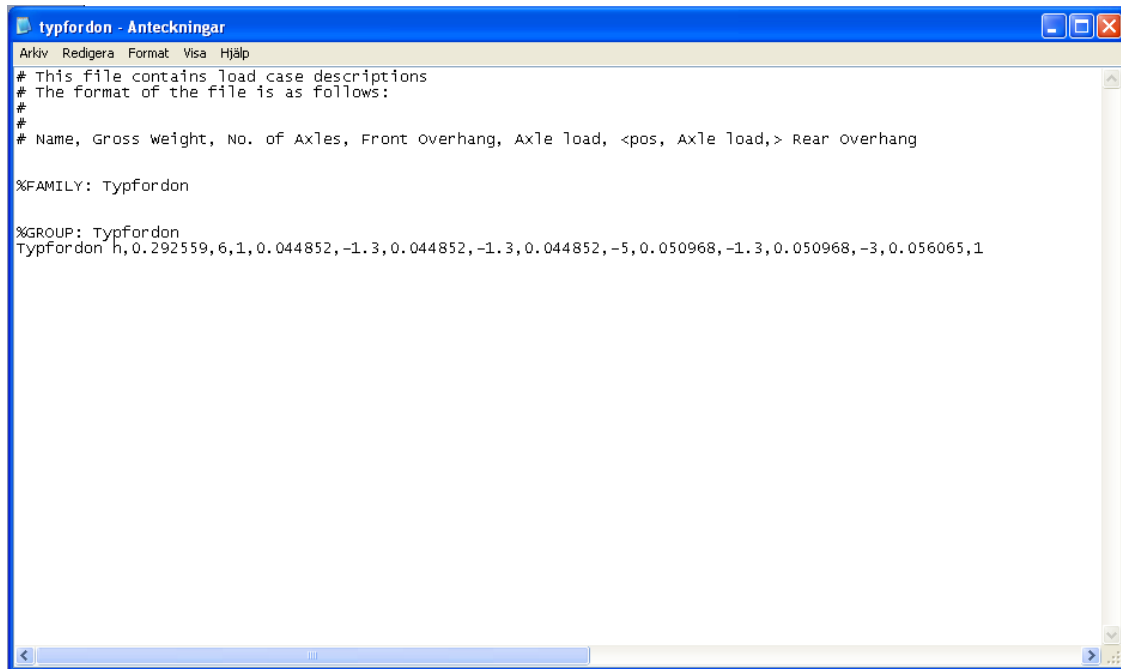
## Appendix B



```
1
vehicle:
Typfordon h)
Axles:
6
Force   Position      width  LoadedLength  Dynamicfactor
0.44    0               1800   200           false
0.44    -1300           1800   200           false
0.44    -2600           1800   200           false
0.5     -7600           1800   200           false
0.5     -8900           1800   200           false
0.55    -11900          1800   200           false
```

The input file to RING2.0 where the force, position, width and loaded length is defined.

## Appendix C



```
typfordon - Anteckningar
Arkiv Redigera Format Visa Hjälp
# This file contains load case descriptions
# The format of the file is as follows:
#
# Name, Gross weight, No. of Axles, Front Overhang, Axle load, <pos, Axle load,> Rear Overhang

%FAMILY: Typfordon

%GROUP: Typfordon
Typfordon h,0.292559,6,1,0.044852,-1.3,0.044852,-1.3,0.044852,-5,0.050968,-1.3,0.050968,-3,0.056065,1
```

The Archie-M input file should contain the loads in tonnes as the program multiplies with  $g$  automatically, but to be able to make a direct comparison with RING2.0 and have the assumed bogie factor  $B$  as 1 kN the design code vehicle h) loads been divided with  $g$ . So the total load from all six axles are

$$\frac{2.87}{9.81} = 0.293$$

Which is the first value after the name in the input file. The other factors on  $B$  is treated in the same way. And the position value is just the space from the last axle.